Published in Chemical Geology 127 : 81-109, 1996,
which should be used for any reference to this work

Evolution of synmetamorphic veins and their wallrocks through a Western Alps transect: no evidence for large-scale fluid flow. Stable isotope, major- and trace-element systematics

C. Henry [a,*], M. Burkhard [a], B. Goffé [b]

[a] *Université de Neuchâtel, Institut de Géologie, 11 rue Émile Argand, CH-2007 Neuchâtel, Switzerland*
[b] *Laboratoire de Géologie, École Normale Supérieure, 24 rue Lhomond, F-75231 Paris Cedex 05, France*

Received 24 May 1994; accepted 31 July 1995 after revision

Abstract

Quartz-rich synfolial veins and wallrocks from different areas of a Western Alps cross-section are examined in an attempt to constrain the scale and mechanisms of fluid flow through metamorphic terrains. Different portions of this cross-section underwent distinct *P–T* evolutions as reflected by the mineralogy of veins: (a) in the greenschist external Dauphinois domain, veins are characterized by quartz and calcite, together with an aluminosilicate (pyrophyllite), Na–K-bearing phyllosilicates and a Fe–Mg-bearing silicate (chlorite); (b) in narrow domains of the Briançonnais and Piémontais zones, with a non-eclogitic HP–LT evolution followed by rapid cooling, veins are characterized by quartz, calcite, Ca- and Fe–Mg-bearing silicates (lawsonite and Fe–Mg-carpholite, respectively); and (c) in the major part of the Briançonnais and Piémontais zones, where low-grade blueschist-facies metamorphism is followed by a greenschist-facies evolution, veins are characterized by the replacement of earlier lawsonite and carpholite by Na- and K-bearing micas. In order to constrain the provenance of fluids involved in vein formation, we determined stable isotope (C, O, H), and major- and trace-element compositions in minerals and whole rocks for a large set of veins and wallrocks. These rocks are compared with some non-metamorphic shales from the northern Paris Basin, considered as protoliths of the Alpine schists.

Stable isotope compositions of calcites are regionally distinct: $\delta^{18}O \approx +28‰$ (SMOW) in the northern Paris Basin, +26‰ in the Briançonnais zone, +22‰ in the Piémontais zone and +18‰ in the Dauphinois zone. Within each studied region, calcite $\delta^{18}O$-values are quite homogeneous regardless of rock type (vein or wallrock). This feature is explained as an isotopic "homogenization" with the most abundant lithology in each zone ("rock-buffered system") — where the overall ratio of calcite (of marine origin) to detrital silicate minerals determines the final isotopic composition of the whole rock (w.r.) after equilibration during Alpine metamorphism. $\delta^{18}O/\delta D$-values of analysed hydrated minerals and whole rocks ($\delta^{18}O \approx +15$ to +25‰ and $\delta D \approx -60‰$ SMOW) lie within the field of Alpine cover rocks and of fluids in equilibrium with these rocks: interaction with an external ^{18}O- or D-depleted fluid, such as hydrothermal waters, meteoric water or "basement fluid", can be ruled out. Major- and trace-element systematics indicate an enrichment in Si, Ca, P, Sr, Y, Ta and locally Eu in the veins with respect to the wallrock, related to massive crystallization of quartz and carbonates, together with phosphate and oxide. Potential fluid sources, chemical composition of the fluid phase and the mechanisms of fluid flow during vein formation are discussed. Fluid flow takes place within tectonic units, at both hectometric and decimetric scale. Fluid may also have migrated along and across the major tectonic contacts but this process is poorly documented.

* Corresponding author. Present address: Université Bordeaux 1, UFR Sciences Terre, Avenue des Facultés, F-33405 Talence Cedex, France.
INA1

1. Introduction

Quartz-rich veins or segregations are an ubiquitous feature in metamorphic rocks of any composition, notably in metapelites and metamarls. Veins have attracted the interest of and been extensively studied by structural geologists (Weiss, 1972; Ramsay and Huber, 1983) and petrologists. Syntectonic, synmetamorphic veins are found in a wide variety of metamorphic terrains ranging from Barrovian (e.g., Yardley, 1983, 1986) to high pressure–low temperature (HP–LT) environments (Rumble and Spear, 1983; Nelson, 1991). Syntectonic (synfolial; Weiss, 1972) veins mostly have a lenticular shape and vary in size from less than a millimetre to several decimetres in thickness, with the longer dimension subparallel to the dominant foliation. Later (syn- to post-tectonic/metamorphic) veins are generally at a high angle to the schistosity and will not be considered here. The most abundant minerals in synfolial veins are quartz and/or carbonates. These minerals are associated with a large variety of other minerals dependent on the wallrock and metamorphic grade (e.g., Kerrick, 1983, chap. 10, with references therein).

In the low- and medium-grade metamorphic conditions considered here, there is overwhelming evidence and a general agreement that the vein-forming minerals have crystallized from a fluid phase, during successive opening/sealing episodes (e.g., Ramsay and Huber, 1983). The study of such veins is thus of prime interest to constrain the scale and mechanisms of fluid and/or solute transport through metamorphic rocks and terrains. Two extreme end-members of possible fluid behaviour exist and are debated at length in the literature (e.g., Fletcher and Hoffmann, 1974; Ferry, 1980; McCaig, 1984, 1988; Baumgartner and Rumble, 1988; Conolly and Thompson, 1989): (1) open-system behaviour with percolation of large amounts of fluids over considerable distances "through entire mountain chains" (e.g., Fyfe et al., 1978; Graham et al., 1983; Ferry, 1986; Grambling, 1986; Kerrich, 1986; Bebout and Barton, 1989, 1993; Oliver, 1992); (2) "closed-system" behaviour at the scale of a geologic formation where the fluid phase is considered as essentially stationary, occupying the pore space. Transport of ionic species in this latter model is thought to be controlled mainly by diffusion of elements and/or limited circulation (re-cycling) of an "internally-flowing" fluid (Wood and Walther, 1986; Goffé et al., 1987; Burkhard and Kerrich, 1988; Philippot and Selverstone, 1991; Goffé and Vidal, 1992; Yardley and Botrell, 1992).

In this study, we examine synfolial veins from different portions of a cross-section through the Western Alps. Particular emphasis is placed on early synfolial veins which formed during the subduction/collision-related non-eclogitic Alpine metamorphism (Goffé, 1996). Three types of metamorphic evolution can be distinguished: (a) a low-grade evolution, always in greenschist facies, occurs in the external domain of the Dauphinois zone (Aprahamian, 1988; Jullien and Goffé, 1993; Goffé, 1996); (b) a cold HP–LT evolution up to low-grade blueschist facies, followed by cooling during the decompression path. This evolution occurs in narrow domains of the Briançonnais and Piémontais zones (Goffé and Velde, 1984; Goffé and Chopin, 1986; Goffé and Vidal, 1992; Goffé, 1996); (c) a HP–LT evolution up to low-grade blueschist facies, followed by isothermal conditions or heating during decompression through the greenschist facies. This evolution occurs in the major part of the Briançonnais and Piémontais zones (Saliot, 1973; Frey et al., 1974; Desmons, 1977; Steen and Bertrand, 1977; Caby et al., 1978; Goffé and Vidal, 1992).

In each domain, the formation of synfolial veins is highly developed in metasediments. In these rocks, the mineralogical content of the veins reflects the *P–T* evolution: (a) in the greenschist domain, veins are characterized by quartz and calcite, together with an aluminosilicate (pyrophyllite), Na–K-bearing phyllosilicates and a Fe–Mg-bearing silicate (chlorite); (b) in the HP–LT cold domain, veins are mainly characterized by quartz, calcite, and Ca- and Fe–Mg-bearing silicates (lawsonite and Fe–Mg-carpholite, respectively); (c) in domains where low-grade blueschist-facies metamorphism is followed by a greenschist-facies evolution, veins are characterized by the replacement of earlier lawsonite and Fe–Mg-carpholite by Na- and K-bearing micas.

To explain the formation of the segregations and their apparent allochemical evolution, the open question is: where did the fluids come from? From the rock itself through dehydration reactions, or from long distances through large-scale fluid transport across the Alpine orogen (compare Burkhard and Kerrich, 1990; Kyser and Kerrich, 1990; McCaig et al., 1990; Marquer and Burkhard, 1992).

Stable isotope (C, O, H), and major, rare-earth element (REE) and other trace-element compositions have been determined in minerals and whole rocks for a large set of syntectonic veins and country rocks in a transect of the Western Alps. Our sampling scheme was designed as an attempt to: (1) detect evidence for fluid flow from the outcrop to the nappe scale; (2) place constraints on the processes of vein formation; and (3) assess the nature and origin of fluids involved during deformation and metamorphism of these non-eclogitic domains of the Alpine belt. In particular, we expected to detect and quantify isotopic disequilibrium relationships among minerals in veins, among different veins and their respective country rocks and thereby to put constraints on the scale and importance of fluid involvement in deformation/metamorphism.

2. Study area

The arc of the Western Alps is classically subdivided into roughly N–S-trending domains according to paleogeographic origin and present-day tectonic position (Fig. 1a). The three metamorphic domains [(a), (b) and (c) above] correspond to or overlay the paleogeographic zones. Samples have been collected in each domain: (a) from the Dauphinois (or External) zone, characterized by greenschist-facies metamorphism; (b) from the Vanoise area in the Briançonnais zone, characterized by cold HP–LT evolution; (c) from Ubaye Valley (Briançonnais zone) and M. Fraitève area (Piémontais zone), characterized by low-grade blueschist-facies evolution followed by greenschist-facies evolution. In addition, we examined three unmetamorphosed shales from the northern Paris Basin considered as non-metamorphic protoliths of the Alpine schists.

The samples have been collected: (1) within the above quoted zones or units, generally far from the main tectonic contacts (Fig. 1b); (2) in zones near or within minor internal tectonic contacts, which are widespread throughout the main units (see Fig. 2a and b).

2.1. *Dauphinois samples*

In the cover series of the external crystalline Pelvoux massif, quartz-rich veins are frequent within Aalenian black shales (Jullien and Goffé, 1993; see also Fig. 2a). Samples have been collected in two distinct areas, north of La Meije massif (Lauzette and Ventelon, A1 in Fig. 1) and south of Grand Châtelard massif (Jarrier and Villarembert, A2 in Fig. 1). The typical assemblage of the segregations is fibrous, syntectonic quartz and calcite as main minerals, together with phyllosilicates. The most abundant phyllosilicates are pyrophyllite, cookeite (Li-bearing chlorite) and Fe-chlorite, associated with phengite ($Si_{3.08-3.13}$), paragonite and locally margarite. Surrounding black schists, rich in organic matter, contain phyllosilicates (Fe-chlorite + phengite ± paragonite ± pyrophyllite ± cookeite), quartz, together with minor calcite, albite (in pyrophyllite-free samples), rutile, hematite and pyrite. In this part of the Dauphinois zone, the mineralogy of the veins and of the surrounding schists shows a prograde, monophased, greenschist-facies Alpine metamorphism, with *P–T* conditions estimated at 1–5 kbar, 270–340°C (Jullien and Goffé, 1993).

2.2. *Briançonnais samples*

In the Briançonnais zone, quartz-rich segregations have been sampled in Upper Cretaceous–Eocene calc schists from Ubaye Valley (B1 in Fig. 1; cf. Michard and Henry, 1988: Maljasset anticline). Segregations are made of the assemblage quartz–calcite–Fe–Mg-carpholite ($Fe_{0.6}Mg_{0.4}Al_2Si_2O_6(OH)_4$), partially replaced by low-Si phengite, paragonite and chlorite. Surrounding calc schists contain calcite and quartz, together with chlorite, low-Si phengite and paragonite, interpreted as the phyllitic breakdown products after Fe–Mg-carpholite, and minor hematite. This mineralogy, both in veins and surrounding wallrock record a HP–LT metamorphic evolution in blueschist facies, with a minimum pressure of 7 kbar for temperatures around 300–350°C (Goffé and Chopin, 1986; Goffé, 1995), followed by a retromorphic evolution under low-grade greenschist-facies conditions.

In the Western Vanoise cover (Chanrossa, B2 in Fig. 1), we sampled a vein in Dogger metapelites, which contains the following paragenesis: calcite, quartz and "fresh" Fe–Mg-carpholite ($Mg_{0.5-0.8}$). Wallrock contains quartz, Fe–Mg-carpholite, pyrophyllite, rutile and organic matter. This mineralogy, both in veins and surrounding schists implies *P–T* conditions of metamorphism re-estimated at a minimum of 9 kbar and 350°C (cf. Vidal et al., 1992). The com-

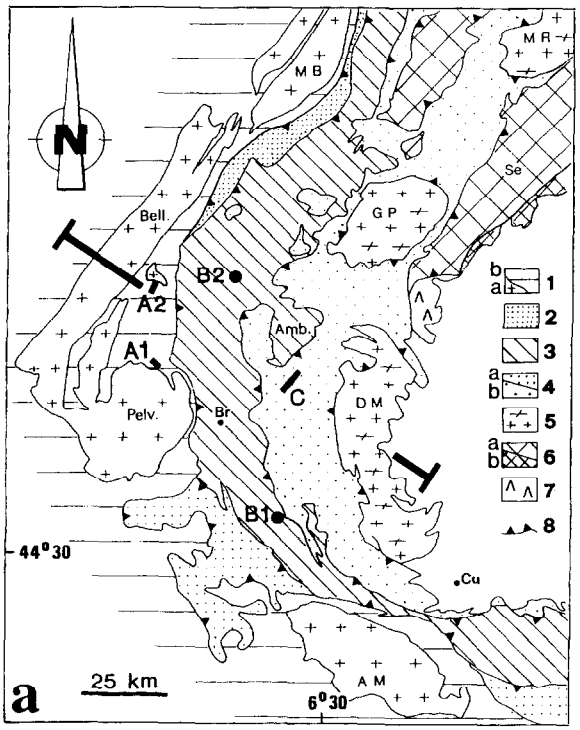

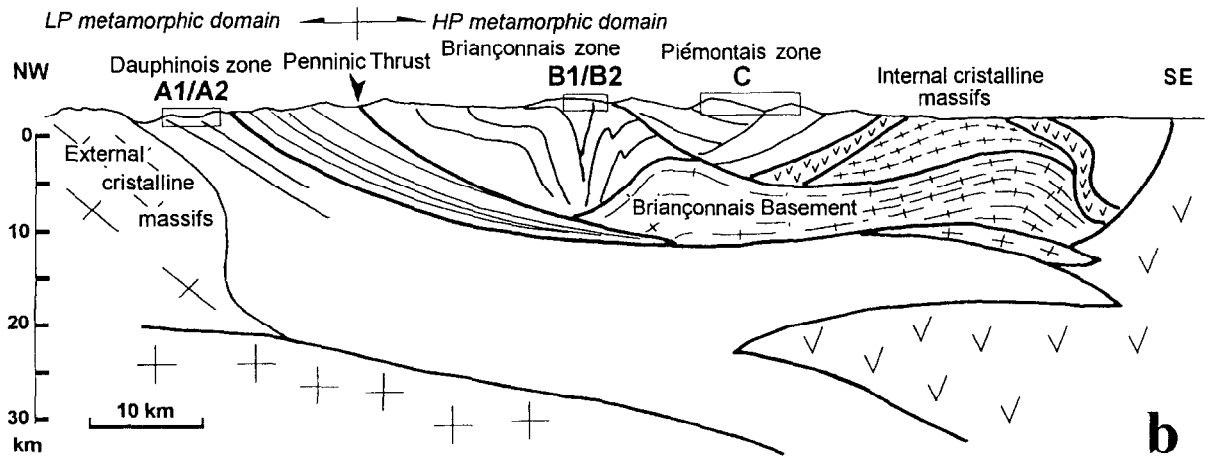

Fig. 1. Geological setting of the studied samples (A1–A2, B1–B2 and C).
a. Map. 1 = Dauphinois–Helvetic external zones (*a* = basement, *b* = cover); 2 = Valaisan zone (Tarentaise breccias); 3 = lower and middle Penninic (Sub-briançonnais and Briançonnais–Grand St Bernard nappes); 4*a* = Helminthoid Flysch, 4*b* = Piémontais zone (Schistes Lustrés metasediments and ophiolitic bodies, undifferentiated); 5 = Internal Penninic massifs; 6*a* = Austro-Alpine nappes, 6*b* = South Alpine domain; 7 = Lanzo ultramafic body; 8 = main thrust contacts. Abbreviations: *AM* = Argentera–Mercantour; *Amb.* = Ambin; *Bell.* = Belledonne; *Br* = Briançon; *Cu* = Cuneo; *DM* = Dora–Maira; *GP* = Gran Paradiso; *MB* = Mont-Blanc; *MR* = Monte Rosa; *Pelv.* = Pelvoux; *Se* = Sesia zone.
b. Schematic cross-section, after Roure et al. (1990) and personal data.

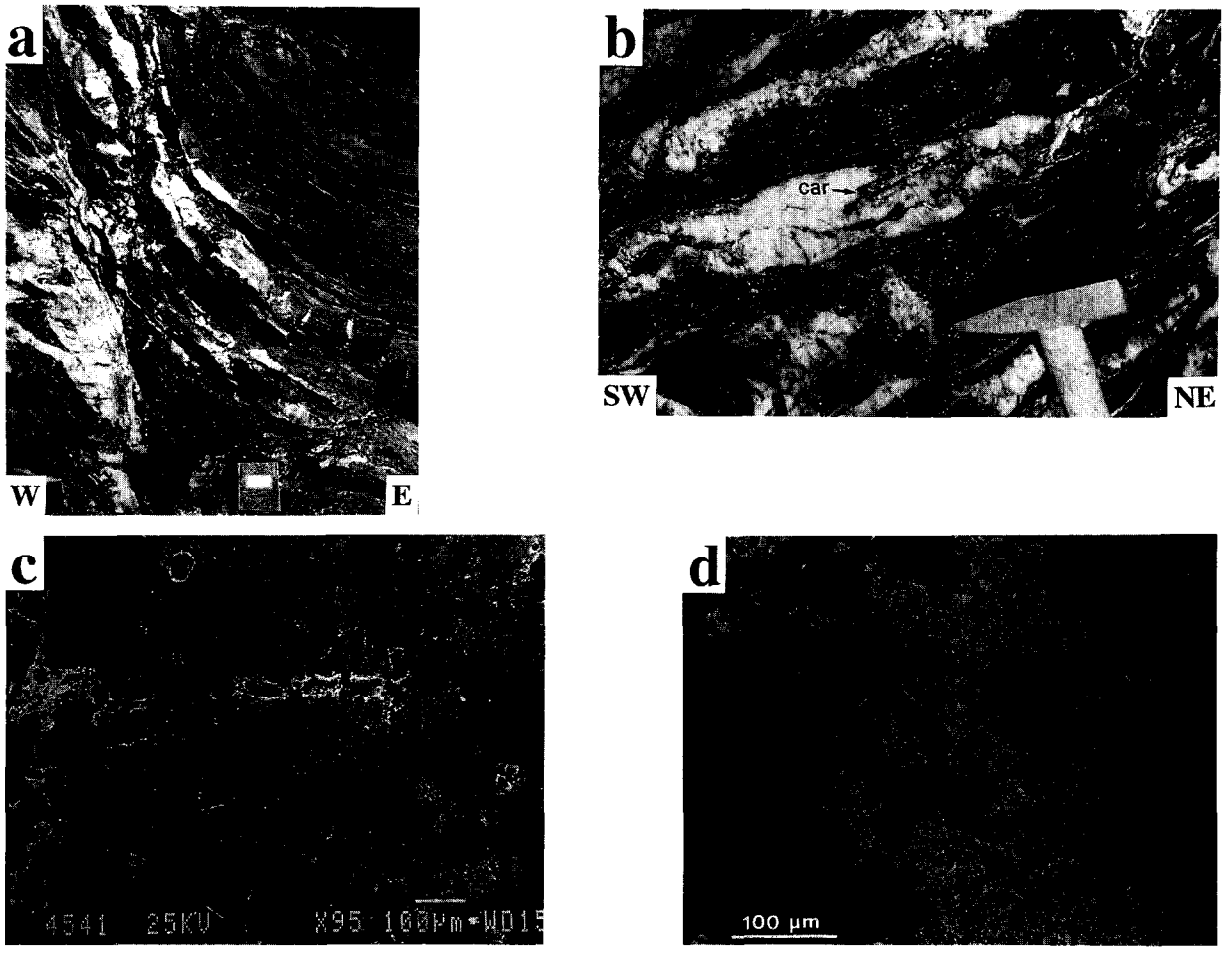

Fig. 2. Aspects of the studied veins at various scales.
a. Cookeite-bearing veins in their black schist wallrock, Dauphinois zone, Villarembert.
b. Fe–Mg-carpholite-bearing veins in their schistose, Fe–Mg-carpholite-bearing wallrock, Piémontais zone, Fraitève area. The regional foliation parallels minor tectonic contacts. *car* = Fe–Mg-carpholite.
c. Micrometric intergrowth of Fe–Mg-carpholite (*light grey*) and quartz (*dark grey*), M. Fraitève. In *white*: Fe-oxides. MEB, BSE image. Note the scale change (b)–(c), which follows a fractal law (see text).
d. Microphotograph of a pseudomorph after Fe–Mg-carpholite by "rosettes" of phyllosilicates (*grey*), Fraitève area. In *black*: quartz. Crossed nicols.

plete preservation of this blueschist-facies paragenesis indicates that retrograde metamorphism was characterized by cooling along a very low geothermal gradient after *P–T* peak (Goffé and Velde, 1984; Gillet and Goffé, 1988).

2.3. *Piémontais samples*

Samples have been collected in the oceanic Schistes Lustrés part of the Piémontais zone, on a SW–NE cross-section between M. Fraitève and M. Genevris (C in Fig. 1). In this area, synfolial veins are abundant in both metapelitic and metamarly layers, which are intimately interbedded at decimetric scale.

In fresh HP–LT minerals bearing-samples, veins contain Fe–Mg-carpholite ($Mg_{0.4-0.5}$) and/or lawsonite + quartz ± calcite ± ankerite. In the veins, Fe–Mg-carpholite is intimately associated with quartz, from (sub)micrometric (Fig. 2c) to decimetric (Fig. 2b) scale. The analysis of the scale variation between quartz

Table 1
Isotopic composition of minerals and rocks from Briançonnais and Dauphinois zones, Western Alps, and from northern Paris Basin

Sample/mineral	$CaCO_3^a$ (% in rock)	$\delta^{13}C$ (‰ vs. PDB)	$\delta^{18}O$ (‰ vs. SMOW)	δD (‰ vs. SMOW)
BRIANÇONNAIS ZONE:				
Ub 873m, Upper Cretaceous-Eocene calc schist, Ubaye Valley:				
Calcite	71	+1.4	+26.0	
Insoluble residue (chl–ph–qz–pa)[b]			+21.0	
Whole rock			+24.6[d]	
Ub 873s, segregation:				
Calcite	54	+1.2	+25.7	
Quartz			+28.1	
Carpholite			+22.0	−41
Van, segregation in Dogger metapelite, Western Vanoise cover:				
Calcite	70	+1.9	+27.9	
Quartz			+28.3	
Carpholite			+25.0	−55
DAUPHINOIS ZONE:				
Vent 4m, Aalenian schist, La Meije cover:				
Insoluble residue (chl–ph–qz–pa ± ru–ab[c])			+14.8	
Vent 4s, segregation:				
Calcite	53.2	−4.4	+18.7	
Quartz			+19.4	
Vila m, Aalenian schist, Gd Châtelard cover:				
Calcite	0.7	−6.1	+17.2	
Insoluble residue (chl–pyr–ph–qz ± pa)			+15.4	
Whole rock			+15.4[d]	
Vila s, segregation:				
Calcite	16.8	−5.5	+18.2	
Chlorite + cookeite			+16.9	
Quartz			+19.4	
Insoluble residue (qz–chl–cook–pyr + ph)			+17.9	
Whole rock			+18.0[d]	−58
Vila 16, segregation:				
Calcite	24.2	−5.4	+18.2	

Sample/mineral	$CaCO_3^a$ (% in rock)	$\delta^{13}C$ (‰ vs. SMOW)	$\delta^{18}O$ (‰ vs. SMOW)	δD (‰ vs. SMOW)
DAUPHINOIS ZONE (cont.):				
Laz 2m, Aelenian schist, La Meije cover:				
Calcite	4.5	−4.7	+19.5	
Insoluble residue (chl–ph–qz–pa ± ab[c])			+16.4	
Whole rock			+16.5[d]	
Laz 2s, segregation:				
Calcite	11.2	−5.2	+17.5	
Quartz			+19.2	
Jar 4m, Aalenian schist, Gd Châtelard cover:				
Calcite	0.9	−5.7	+17.7	
Insoluble residue (chl–ph–qz ± ru–ab[c])			+13.8	
Whole rock			+13.8[d]	
Jar 4s, segregation:				
Calcite (± ankerite?)	33.6	−5.4	+17.7	
Quartz			+19.6	
Jar soc, Gd Châtelard metagranite:				
Calcite	6.6	−6.2	+14.2	
Insoluble residue (qz–ab–ph–chl)			+13.1	
Whole rock			+13.2[d]	
NORTHERN PARIS BASIN (presumable protolith):				
Arg 1, middle Portlandian shale, Wimereux:				
Calcite	11.5	+0.7	+27.7	
Insoluble residue (gl ± mu–kaol–chl–qz ± f)			+16.5	
Whole rock			+17.8[d]	−65
Arg 2, mid. Portlandian shale, Wimereux:				
Calcite	6.9	+0.3	+27.3	
Insoluble residue (gl ± mu–kaol–chl–qz ± f)			+15.4	
Whole rock			+16.2[d]	
Arg 4, Albian shale, Wissant:				
Calcite	16.5	+2.0	+27.9	
Insoluble residue (gl ± mu–kaol–chl–qz ± f)			+18.3	
Whole rock			+19.9[d]	

[a]Calculated by volumetric determination of CO_2 yield in acid digestion.
[b]In HCl-insoluble residue, minerals are quoted in order of their abundance (ab = albite; chl = chlorite; cook = cookeite; f = undifferentiated feldspars; gl = glauconite; kaol = kaolinite; mu = muscovite; pa = paragonite; ph = low-Si phengite; pyr = pyrophyllite; qz = quartz; ru = rutile).
[c]Phases present in minor amount, only detected by XRD.
[d]Calculated by material balance, from insoluble residue and coexisting calcite.

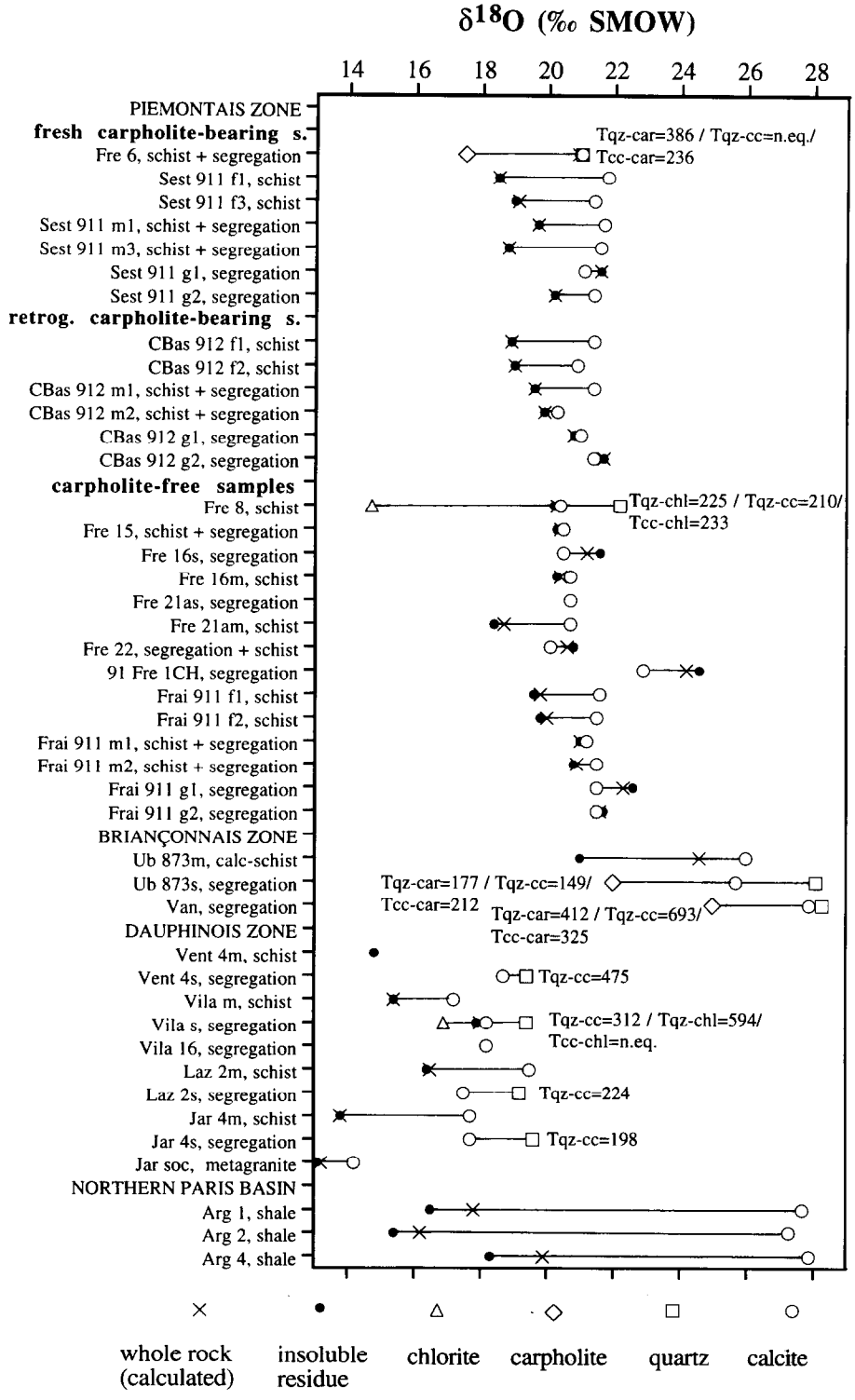

Fig. 3. Oxygen isotopic fractionation between minerals in the studied samples. Temperatures (°C) are calculated using isotopic fractionation equations from Zheng (1991, 1993a, b), with $l\text{-}^{18}O_{(Fe\text{-}Mg\text{-}carpholite)} = 0.8428$ (Y.F. Zheng, pers. commun., 1994). $\delta^{18}O_{(whole\ rock)}$ is calculated by material balance, from insoluble residue and coexisting calcite.

Table 2
Isotopic composition of minerals and rocks from the M. Fraitève area, "Schistes Lustrés" zone, Western Alps

Sample/mineral	$CaCO_3$[a] (% in rock)	$\delta^{13}C$ (‰ vs. PDB)	$\delta^{18}O$ (‰ vs. SMOW)	δD (‰ vs. SMOW)
PRESERVED CARPHOLITE-BEARING SAMPLES:				
Fre 6, *schist + segregation*:				
Quartz			+21.0	
Carpholite			+17.5	−46
Calcite	3.4	−0.7	+21.0	
Insoluble residue (qz–car–wm–ab[a])[b]			+20.9	
Whole rock			+20.9[d]	−60
Sest 911 *f3*, *schist*:				
Calcite	1.5	−4.5	+21.8	
Insoluble residue (chl–wm–qz–car–ab–ru)			+18.5	
Whole rock			+18.5[d]	−60
Sest 911 f3, schist:				
Calcite	1.3	−4.2	+21.4	
Insoluble residue (chl–wm–qz–car–ab–ru)			+19.0	
Whole rock			+19.1[d]	
Sest 911 *m1*, *schist + segregation*:				
Calcite	1.5	−4.1	+21.7	
Insoluble residue (qz–chl–wm–car–ab ± ru)			+19.7	
Whole rock			+19.7[d]	
Sest 911 *m3*, *schist + segregation*:				
Calcite	1.5	−4.3	+21.6	
Insoluble residue (qz–chl–wm–car–ab ± ru)			+18.8	
Whole rock			+18.8[d]	
Sest 911 *g1*, *segregation*:				
Calcite	2.7	−5.3	+21.1	
Insoluble residue (qz–chl–car–wm–ab)			+21.6	
Whole rock			+21.6[d]	
Sest 911 *g2*, *segregation*:				
Calcite	3.9	−4.2	+21.4	
Insoluble residue (qz–chl–car–wm–ab)			+20.2	
Whole rock			+20.2[d]	
CARPHOLITE-FREE SAMPLES:				
Fre 8, *lawsonite-bearing schist*:				
Quartz			+22.2	
Chlorite			+14.7	−64
Calcite (+ ankerite)	49.6	+0.6	+20.4	
Insoluble residue (chl–qz ± wm)			+20.2	
Whole rock			+20.3[d]	−55

Sample/mineral	$CaCO_3$[a] (% in rock)	$\delta^{13}C$ (‰ vs. PDB)	$\delta^{18}O$ (‰ vs. SMOW)	δD (‰ vs. SMOW)
RETROGRESSED CARPHOLITE-BEARING SAMPLES:				
CBas 912 *f1*, *schist*:				
Calcite	0.9	−6.1	+21.4	
Insoluble residue (chl–wm–qz–ru–ab[a])			+18.9	
Whole rock			+18.9[d]	−57
CBas 912 *f2*, *schist*:				
Calcite	0.9	−6.3	+20.9	
Insoluble residue (chl–wm–qz–ru–ab[a])			+19.0	
Whole rock			+19.0[d]	
CBas 912 *m1*, *schist + segregation*:				
Calcite	0.8	−5.8	+21.4	
Insoluble residue (qz–chl–wm–ru–ab[a])			+19.6	
Whole rock			+19.6[d]	
CBas 912 *m2*, *schist + segregation*:				
Calcite	1.0	−6.2	+20.3	
Insoluble residue (qz–chl–wm–ru–ab[a])			+19.9	
Whole rock			+19.9[d]	
CBas 912 *g1*, *segregation*:				
Calcite	1.0	−5.7	+21.0	
Insoluble residue (qz–chl–wm–ru–ab[a])			+20.8	
Whole rock			+20.8[d]	
CBas 912 *g2*, *segregation*:				
Calcite	1.5	−5.9	+21.4	
Insoluble residue (qz–chl–wm–ru–ab[a])			+21.7	
Whole rock			+21.7[d]	
CARPHOLITE-FREE SAMPLES (cont.):				
91 *Fre* 1*CH*, *segregation*:				
Calcite	26.0	−0.5	+22.9	
Insoluble residue (qz–ab[a])			+24.6	
Whole rock			+24.2[d]	

Table 2 (*continued*)

Sample/mineral	$CaCO_3$[a] (% in rock)	$\delta^{13}C$ (‰ vs. PDB)	$\delta^{18}O$ (‰ vs. SMOW)	δD (‰ vs. SMOW)
Fre 15, *lawsonite-bearing schist + segregation*:				
Calcite	52.0	−2.3	+20.5	
Insoluble residue (qz–chl–wm)[b]				20.3
Whole rock			+20.4[d]	
Fre 16*s*, *segregation*:				
Calcite	39.0	−1.8	+20.5	
Insoluble residue (qz–wm–chl–ab[c])			+21.6	
Whole rock			+21.2[d]	
Fre 16*m*, *schist*:				
Calcite	26.0	+1.9	+20.7	
Insoluble residue (chl–wm–qz–ab[c] ± ru)			+20.3	
Whole rock			+20.4[d]	
Whole rock			+20.9[d]	
Fre 21*as*, *segregation*:				
Calcite	16.0	+0.32	+0.7	
Fre 21*am*, *schist*:				
Calcite	13.0	+0.62	+0.7	
Insoluble residue (chl–wm–qz–ab[c])			+18.4	
Whole rock			+18.7[d]	
Fre 22, *segregation + schist*:				
Calcite	30.0	+0.32	+0.1	
Insoluble residue (wm–chl–qz–ab[c])			+20.8	
Whole rock			+20.6[d]	
Frai 911 *f1*, *schist*:				
Calcite	12.0	−0.6	+21.6	
Insoluble residue (chl–wm–qz–ab–ru)			+19.6	
Whole rock			+19.8[d]	−66
Frai 911 *f2*, *schist*:				
Calcite	11.4	−0.6	+21.5	
Insoluble residue (chl–wm–qz–ab–ru)			+19.8	
Whole rock			+20.0[d]	
Frai 911 *m1*, *schist + segregation*:				
Calcite	18.5	−0.8	+21.2	
Insoluble residue (qz–chl–wm–ab ± ru)			+21.0	
Whole rock			+21.0[d]	
Frai 911 *m2*, *schist + segregation*:				
Calcite	19.8	−0.6	+21.5	
Insoluble residue (qz–chl–wm–ab ± ru)			+20.8	
Frai 911 *g1*, *segregation*:				
Calcite	29.4	−0.5	+21.5	
Insoluble residue (qz–ab–chl ± wm)			+22.6	
Whole rock			+22.3[d]	
Frai 911 *g2*, *segregation*:				
Calcite	28.0	−0.6	+21.5	
Insoluble residue (qz–ab–chl ± wm)			+21.7	
Whole rock			+21.6[d]	

[a]Calculated by volumetric determination of CO_2 yield in acid digestion.

[b]In HCl-insoluble residue, minerals are quoted in order of their abundance (ab = albite; car = carpholite; chl = chlorite; qz = quartz; ru = rutile; wm = phengitic and paragonitic white micas).

[c]Phases present in minor amount, only detected by XRD.

[d]Calculated by material balance, from insoluble residue and coexisting calcite.

and Fe–Mg-carpholite shows that these minerals grew in a fractal form. The measure of the fractal dimension gives a D-value of ~ 1.7 (Agard and Cuny, 1992); it is compatible with a diffusion-limited aggregation (DLA) process in a fluid phase (Falconer, 1990). Surrounding schist is composed of Fe–Mg-carpholite and/or chloritoid and/or lawsonite porphyroblasts in a foliated matrix of quartz, organic matter, hematite, rutile, together with more or less abundant carbonates, chlorite and minor white micas. This mineralogy, both in veins and surrounding schists, implies a low-grade blueschist-facies metamorphic evolution, with P–T conditions of ~ 7 kbar, ~ 350°C, followed by cooling during the decompression path. These "fresh" samples occur only at the top of the M. Fraitève.

In altered samples, veins are made of quartz + calcite ± ankerite, together with Fe–Mg-carpholite and/or lawsonite partly or totally pseudomorphosed by "rosettes" (e.g., Fig. 2d) of white micas (paragonite + phengite $Si_{3.3-3.5}$) + chlorite ± albite (often twinned) ± calcite ± hematite ± rutile. Texturally, two types of quartz are distinguishable and can coexist within these segregations: (1) up to 10 cm in length, slightly undulose HP monocrystalline quartz intimately associated with Fe–Mg-carpholite relics, which appears as very tiny needles included in it; (2) secondary lobate quartz, often intimately associated with chlorite and white micas; this quartz corresponds to LP metamorphic evolution. The late, Fe-rich chlorite frequently develops as up to 100×500-μm size typical vermicular crystals, that assemble into centimetric patches. Surrounding metapelitic to metamarly wallrock is made of quartz, calcite, white micas, chlorite and organic matter, together with subordinate pyrite, rutile and hematite; relics of lawsonite or Fe–Mg-carpholite are locally observed. The mineralogical assemblages found, both in veins and in wallrocks, indicate a low-grade blueschist-facies metamorphic evolution with P–T conditions of ~ 7 kbar, ~ 350°C, followed by a greenschist-facies overprint characterized by decompression with a slight increase in temperature (Goffé and Vidal, 1992). These altered samples occur at the base of M. Fraitève and everywhere toward M. Genevris.

2.4. Non-metamorphic shales from the northern Paris Basin

Three shaly samples have been collected from Upper Jurassic–Cretaceous cliffs of the northern Paris Basin (Boulogne-sur-Mer area): mid-Portlandian "Exogyra marls" near Wimereux and Albian "plastic shales" near Wissant. These non-metamorphic samples contain the assemblage quartz + calcite + micas + glauconite + kaolinite + chlorite ± feldspars. These rocks can be considered as close analogues or "protoliths" of the Alpine, metamorphosed metapelites and metamarls (Brosse, 1982).

3. Analytical techniques

3.1. Sampling and sample preparation

In order to characterize the different types of veins and country rocks from each area, two kinds of samples have been collected: (1) hand-specimen of either vein, wallrock, or a mixture of both; (2) "geochemical" samples, i.e. up to 30 kg of whole rock (mixture of vein and schist), corresponding to a unique slice of rock of ca. 0.40 m × 0.20 m × 0.15 m, taken off perpendicularly to the main mylonitic foliation, and which can be considered as representative of the "average deformed lithology" in the considered area. This second type of sample has only been collected in the Piémontais zone (samples Sest911, CBas912 and Frai911 in Table 2).

Hand-specimens were finely powdered in a tungsten carbide disc mill after manual separation of the vein material from schistose host rocks.

The 30-kg samples were first roughly crushed in a jaw crusher to a grain size of $\sim$0.2–1 cm. These crushed whole-rock samples were then separated into three fractions of distinct grain sizes: (1) a coarse fraction, with a grain size of 0.5–1 cm, which has been considered as representative of the massive segregation, with very minor contamination by schist; these samples are referred to as "segregations" or "veins" in the following; (2) a medium fraction, with intermediate grain size of 0.2–0.5 cm, which can be considered as approximately representative of the whole rock (mixture of segregation and schist); and (3) a fine fraction, with a maximal grain size of 0.2 cm, which

has been considered as representative of the cleavable wallrock schist, with very minor contamination by vein; these samples are referred to as "country rock" or "wallrock" in the following. Each of these three fractions was homogeneously mixed and split into three or four precisely weighed "sub-samples", termed g, m and f for segregation (vein), whole rock and schist (wallrock), respectively (see Tables 2–5). Sub-samples were finally powdered to a maximal grain size of ~ 100 μm, before specific preparations for different analyses.

3.2. *Mineral separation*

Carbonate-free "insoluble residues" were obtained by dissolution of powdered samples in a 10–20% HCl solution, followed by extensive rinsing prior to analysis. The silicate minerals quartz, chlorite and Fe–Mg-carpholite were isolated from each other and from other minerals by repeated heavy-liquid separation using a sodium polytungstate (NaPT) solution at 2.62, 2.7 and 2.9 g cm^{-3}, respectively, in a thermostatized centrifuge (2400*g*) for 15–30 min. The mineralogical composition of separates was monitored by X-ray diffraction (XRD) and improved manually under binoculars; the separates generally contain $<5\%$ of remaining secondary minerals.

3.3. *Stable isotope analyses*

Stable isotope extractions were performed at the University of Saskatchewan, Canada (O, C and H on carbonates and silicates) and at the University of Lausanne, Switzerland (O and C on carbonates).

O and C extraction: Standard procedures, using 100% H_3PO_4 at 25°C on whole-rock powders were applied for CO_2 extraction from calcites (McCrea, 1950). Standard procedures using BrF_5 (Clayton and Mayeda, 1963) were employed for the extraction of O_2 from silicate minerals and insoluble residues.

H extraction: After an initial drying period of several hours at 110°C to remove adsorbed water from the fine-grained sheet silicates, hydrogen was extracted from hydroxysilicates at 1400–1500°C, oxidized to H_2O with ZnO and reduced to hydrogen over uranium at 800°C (Savin and Epstein, 1970).

Carbon, oxygen and hydrogen isotopic compositions were determined on a Finnigan® MAT 251 mass spectrometer. Isotopic data are reported in the standard δ notation, as ‰ deviations from SMOW (standard mean ocean water) for oxygen and hydrogen, and from PDB (Peedee belemnite) for carbon. The long-term reproducibilities (2σ) are ± 0.2‰ for δ^{18}O- and δ^{13}C-values, and ± 2‰ for δD-values.

3.4. *Major-, trace- and rare-earth element analyses*

Major oxide compounds of rock samples were determined at the École Normale Supérieure Paris, France, by standard wet chemical methods (alkaline fusion and colorimetry for SiO_2 and Al_2O_3; acid attack with titration for Fe_2O_3 and FeO; atomic absorption for MnO, MgO and CaO; flame spectrometry for Na_2O and K_2O; acid attack and colorimetry for P_2O_5 and TiO_2; Penfield tube method with heating at 1500°C for total H_2O; and double weighing with heating at 900°C for loss on ignition (LOI), with granite MA-N GIT-IWG as IAGC standard; Govindaraju, 1984).

Hot digestion of ~ 0.1 g of rock sample in a mixture of HNO_3 and HF was performed before inductively coupled plasma–mass spectrometric (ICP–MS) analyses of a large set of trace elements (REE, Be, Li, Mo, Nb, Ta, V, Zr, Sc, Hf, Y, U, Sr, Th, Pb, Bi, Ba, Tl, Rb, Cs), at the University of Saskatchewan, Canada. Accuracy and precision range from $< \pm 3\%$ to $\pm 7\%$ for the analyzed trace elements (Jenner et al., 1990).

4. Results and discussion

4.1. *Oxygen partitioning between minerals: test for isotopic equilibrium*

Stable isotope values for minerals, insoluble residues and whole rocks are summarized in Table 1 and Table 2, and Fig. 3. Assuming isotopic equilibration under greenschist-facies conditions among minerals in any given rock sample, the following order of minerals with decreasing δ^{18}O-values has to be expected, according to the theoretical calibrations of Zheng (1993a, 1993b): quartz, calcite, albite, phengite/anorthite/muscovite, chlorite, pyroxene, amphibole, oxides; this is slightly different from the order previously given by Faure (1986, chap. 25) and Frey et al. (1976) — particularly for chlorite — because their order was based on the observation from natural assemblages

which may have experienced isotopic re-equilibration during cooling. In most of the studied samples, this general order is respected, suggesting that the analyzed minerals have indeed approximated isotopic equilibrium with regard to oxygen. δ^{18}O-values for insoluble residues vary as a function of the composition of the residue: values lower than those of coexisting calcite are obtained for phyllite-dominated samples (schist and schist + segregation), values similar to those of coexisting calcite, and/or slightly higher ones are obtained for quartz-rich samples (mostly segregations). This order has to be a result of Alpine metamorphism because the minerals in the protolith were certainly not grouped in this order (compare for instance the Paris Basin samples or data from the literature: e.g., Faure, 1986; Hoefs, 1987; Kyser, 1987). In all the analysed rocks, calcite has marine origin and therefore a presumable initial δ^{18}O-value of +27 to +30‰ SMOW. Quartz, on the other hand, is mostly of detrital origin with an estimated average "crustal-metamorphic" δ^{18}O-value of +8 to +15‰. Phyllosilicates of detrital origin had an initial, either "sedimentary" high δ^{18}O-value (compare Faure, 1986; Hoefs, 1987; Kyser, 1987), or a "basement-derived" low value (e.g., Bouquillon et al., 1990); as "basement-derived", detrital micas partly re-equilibrate during sedimentary processes, the phyllosilicate fraction most probably had an initial average "sedimentary" value of +15 to +20‰ SMOW.

From the present observation that these initial, detrital/sedimentary values have been completely obliterated, it is obvious that isotopic re-equilibration among the rock-forming minerals must have taken place during diagenesis and Alpine metamorphism. More detailed examination, however, reveals many instances where minerals did not attain perfect isotopic equilibrium for presumable Alpine metamorphic temperatures, as outlined by abnormal temperatures in Fig. 3. Isotopic temperatures have been calculated using the theoretical calibrations of Zheng (1991, 1993a, 1993b). For Fe–Mg-carpholite, Y.F. Zheng (pers. commun., 1994) has calculated an I-^{18}O index of 0.8428 and obtained the following fractionation factor equations for the quartz–carpholite, calcite–carpholite and carpholite–water systems, respectively:

$$10^3 \ln \alpha_{qz-car} = 0.32 \cdot 10^6/T^2 + 2.51 \cdot 10^3/T - 1.04$$

$$10^3 \ln \alpha_{cc-car} = -0.15 \cdot 10^6/T^2 + 2.61 \cdot 10^3/T - 1.04$$

$$10^3 \ln \alpha_{car-w} = 4.16 \cdot 10^6/T^2 - 7.27 \cdot 10^3/T + 2.20$$

Possible sources for deviations from perfect isotopic equilibrium are as follows:

(1) This is the first stable isotope (δ^{18}O and δD) analysis of Fe–Mg-carpholites, and accordingly, no fractionation factors for this mineral are available. Fe–Mg-carpholite is a hydrated aluminosilicate with a single-chain, pyroxene-like structure (McGillavry et al., 1956; Viswanathan, 1981; Ferraris et al., 1992). The measured fractionation of 3–6‰ between Fe–Mg-carpholite and quartz lies in the range expected for pyroxenes and/or amphiboles in blueschist- or greenschist-facies metamorphism. Using fractionation curves of Y.F. Zheng (pers. commun., 1994; see above), some isotopic disequilibrium is outlined: the lowest values of 3.5‰ (sample Fre6) and 3.3‰ (sample Van) yield reasonable temperatures (i.e. 386° and 412°C, respectively), whereas the highest fractionation of 6.1‰ (sample Ub873) clearly yields apparently a too low isotopic temperature (i.e. 177°C) for blueschist- or greenschist-facies metamorphism. This discrepancy could be the result of a selective resetting of quartz related to its recrystallization. (A resetting of the carpholite isotopic composition during later greenschist-facies metamorphism seems very unlikely.)

(2) Isotopic disequilibrium relations are obvious from the calculation of the isotopic temperature in a few samples (see Fig. 3). In the Piémontais zone, realistic isotopic temperatures of ~225°C are calculated from quartz–calcite, quartz–chlorite and calcite–chlorite fractionations (sample Fre8). As chlorite indicates the greenschist-facies evolution, these isotopic temperatures are probably related to this later event, although relics of a HP–LT event are present in the sample. The disequilibrium among quartz and calcite observed in Fre6 could be explained by only partial recrystallisation of quartz during greenschist-facies metamorphism; HP and LP quartz are distinguishable in thin section by characteristic textures (see Section 2.3) — physical separation of these two quartz populations for isotopic analysis is impossible. In the Briançonnais and Dau-

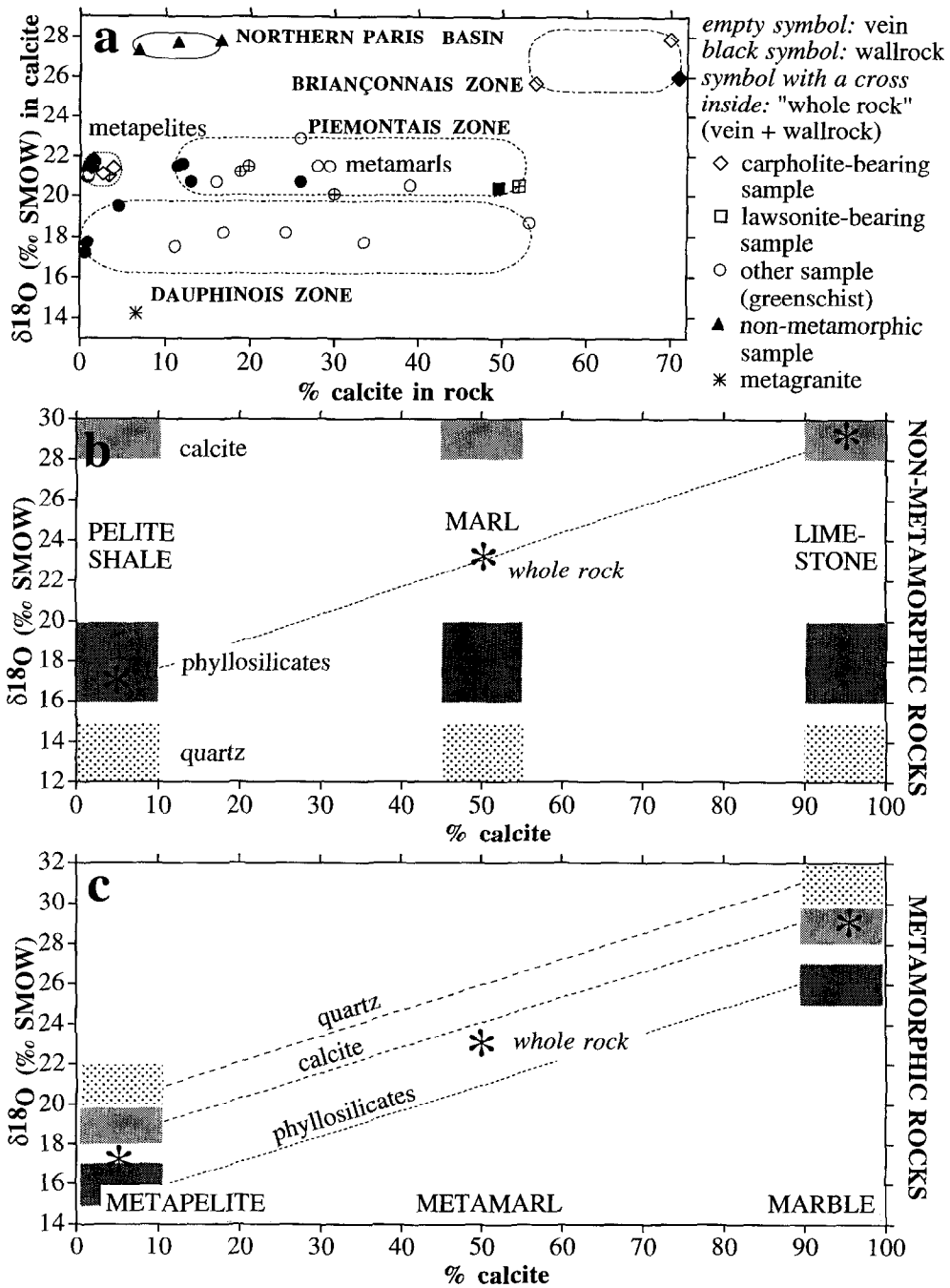

Fig. 4. $\delta^{18}O$-values of minerals vs. calcite content in rock.
a. Systematics for calcite in the studied samples.
b. Schematic evolution in non-metamorphic rocks.
c. Schematic evolution in metamorphic rocks, inspired by Gregory and Criss (1986).

phinois zones, O partitioning between quartz and calcite indicates correct greenschist-facies temperatures in some segregations (Vilas and Laz2s), whereas either too high or too low temperatures indicate O disequilibrium in other segregations (Vent4s and Jar4s, respectively). From the data exposed above, we conclude, that on the whole, and in each studied zone, the observed O-isotopic values in minerals (except in HP Fe–Mg-carpholite and partially in coexisting quartz) were acquired during a greenschist-facies stage. More specifically, calcite δ^{18}O-values were acquired during greenschist-facies metamorphism in all samples: their comparison is thus facilitated and can inform us about the nature of the fluid phase present during the LP metamorphic evolution.

4.2. *δ^{18}O calcite vs. calcite content in the sample*

In Fig. 4a, calcite δ^{18}O-values are plotted vs. the calcite content in the studied samples. The most striking results are the following: (1) in each region studied, calcite δ^{18}O-values, regardless of the type of sample, are quite homogeneous, varying by no more than ± 1.5‰; (2) regionally characteristic δ^{18}O-values for calcite are clearly distinct from one region to another: δ^{18}O (‰ SMOW) of $\sim +28$‰ are found in the northern Paris Basin, $\sim +26$‰ in the Briançonnais zone, $\sim +22$‰ in the Piémontais zone and $\sim +18$‰ in the Dauphinois zone. Both the regional homogeneity of calcite composition with respect to δ^{18}O, regardless of the rock type, and the characteristic composition for each tectonic unit, are remarkable and require an explanation.

Calcite in whole rocks (pelites, marls, limestones) has a marine origin and ought to have initially enriched δ^{18}O-values. However, as pointed out above, the rock-forming minerals quartz, phyllosilicates and calcite, albeit of different relative proportion in the different rocks, have approached isotopic equilibrium during Alpine deformation and metamorphism. If this metamorphism took place in a "closed system" (i.e. rock $\pm$ a fluid phase in equilibrium), the isotopic composition of the whole rock must have remained unchanged, (compare stars in Fig. 4b and c), whereas individual minerals underwent large changes in isotopic composition, especially quartz and calcite which have to shift in opposite directions (Gregory and Criss, 1986). This behaviour is sketched in Fig. 4b and c. The original isotopic composition of the three main constituent minerals are indicated with different gray shaded boxes. The relative abundance of the calcite is reported on the x-axis — this factor has the largest influence on the whole-rock isotopic composition of the different rock types. In the case of a pelite or shale (Paris Basin samples), the calcite δ^{18}O-value is high as expected for a marine origin; however, given the small percentage of this mineral in the rock, the δ^{18}O whole-rock composition is dominated by that of the abundant phyllosilicates. The sketched situation of Fig. 4c applies directly to the observed trends within the different tectonic units (Dauphinois, Briançonnais, Piémontais). Rather than calcite content of the hand-specimen, i.e. on the 10–20-cm scale, the average whole-rock calcite content at the scale of each tectonic unit (~ 500 m?) seems to be responsible for the regionally constant δ^{18}O-values as measured in calcite: < 10 wt% $CaCO_3$ in the studied part of Dauphinois zone, ~ 30% in the Piémontais zone and > 80% in the Briançonnais cover.

The Briançonnais zone is dominated by a thick series of platform carbonates of Middle to Late Triassic age, and by a thin Mesozoic to Cenozoic carbonate series, with rare marly interlayers and virtually no siliciclastics. In the Vanoise area, the Fe–Mg-carpholite-bearing samples stem from volumetrically negligible thin metapelitic horizons (0.1–3 m), Dogger in age (Ellenberger, 1958). In the Ubaye Valley, Fe–Mg-carpholite is present in a thin Eocene calc-schist series, located at the top of the carbonate series. In accordance with the carbonate dominance in the Briançonnais zone, Fe–Mg-carpholite-bearing segregations and country rocks have high δ^{18}O-values.

In the M. Fraitève area of the Piémontais zone, characterized by alternate layers of metapelites and metamarls at decimetric scale (e.g., Caron, 1977), calcites from both metapelitic and metamarly layers display the same δ^{18}O-values. Calcites from metapelites show "too high" δ^{18}O with respect to those expected, whereas the most carbonate-rich metamarls show clearly "too low" calcite δ^{18}O-values. This is interpreted as an "isotopic equilibration" among the different layers, at least where calcite is concerned. Such an equilibration, although not perfectly attained, was certainly facilitated by the presence of a fluid phase which also lead to the abundant Fe–Mg-carpholite–quartz–calcite segregations.

In the Dauphinois zone, the Aalenian black shale represents the least carbonate-rich rock of all analysed samples. Carbonates do occur, however, mainly in segregations, together with quartz and phyllosilicates. Calcites exhibit low δ^{18}O-values, in good agreement with those expected for this shale-dominated environment. Furthermore, the homogeneous low calcite δ^{18}O-values indicate that the Aalenian "shale system" was not connected to the overlying Dauphinois carbonate series.

In conclusion, calcite δ^{18}O-values in whole rocks, segregations and their country rocks seem to be controlled by that of the most abundant lithology in each zone. This finding is interpreted as a "closed-system behaviour", or a "buffered system" (infinite isotopic reservoir) on the scale of formations (e.g., Aalenian black shales or Piémontais "Schistes Lustrés"). This behaviour indicates that the system is connected at the formation scale, and that each formation is "isotopically isolated" from the surrounding ones (e.g., Aalenian black shales). Accordingly, any fluid — infiltrating or internal — would have had its isotopic composition buffered by the local rock sequence, which is an indication of low water/rock ratios (e.g., Bröcker et al., 1993).

4.3. Regional variations in calcite C/O systematics

δ^{18}O- vs. δ^{13}C-values for calcites are represented in Fig. 5a. This figure shows the distinct δ^{18}O-value in each studied zone (as discussed above). δ^{13}C-values show some characteristic trends for each zone: invariably high values of $+1$ to $+2$‰ (PDB) are found in the Briançonnais zone, a large scatter of values between ~ -6 and $+2$‰ is present in the Piémontais zone, whereas consistently low values of -6 to -4.5‰ prevail in the Dauphinois zone.

A comparison of stable isotope data compiled from the literature for calcites from different areas of the Western and Central Alps (Fig. 5b–d) shows the following trends:

(1) In the carbonate-dominated Briançonnais zone (Fig. 5c), stable isotope composition, regardless of provenance and metamorphic grade, cluster tightly at high δ^{13}C- and high δ^{18}O-values, typical for marine carbonates. No signs of depletion due to Alpine metamorphism and/or interaction with metamorphic fluids from surrounding tectonic units or late Alpine meteoric waters can be detected in this data set (compare Kerrich, 1987; Burkhard and Kerrich, 1990; Burkhard et al., 1992).

(2) The Piémontais (Fig. 5b) and External zones (Fig. 5d), on the contrary, both display larger dispersal in isotopic compositions with two types of trends of depletion in ^{18}O (vertical trend) and ^{13}C (horizontal trend), respectively. Both trends can be interpreted as modifications of an initial marine composition through interaction with a rock or fluid reservoir of distinct isotopic composition.

Abnormally low δ^{18}O-values are explained by the interaction of the rock with an external, ^{18}O-depleted fluid, either hydrothermal waters (e.g., 4 and 6 in Fig. 5b), metamorphic fluids in equilibrium with (metamorphic) basement (e.g., 6 in Fig. 5d and M in Fig. 5e), or a meteoric fluid. An abnormally high value of calcite in the Dauphinois metagranite could be interpreted as the result of the reverse trend, i.e. infiltration of an ^{18}O-enriched "sedimentary fluid" into the basement.

^{13}C depletion is commonly interpreted as the result of "interaction with organic matter" and/or an "organic fluid" (Sheppard, 1986). ^{13}C-depleted samples are systematically associated with layers rich in organic matter (veins 2 and 4A in Fig. 5b and d, respectively; see also Baker, 1990). The Piémontais zone samples illustrate this clearly: marly, carbonate-rich samples with certainly low organic carbon content yield almost "marine" calcite δ^{13}C-values, whereas wallrock and segregation calcite from black metapelites with higher organic material content yield the lowest δ^{13}C-values — in the same range as those found in Aalenian black shales from the Dauphinois zone and other areas of the Alps (Fig. 5d). This clear shift in δ^{13}C compositions between metapelitic and metamarly beds, which are interlayered at decimetric scale, results from preferential re-equilibration of calcite and indicates local interaction with organic matter in the metapelites. A concomitant lowering of δ^{13}C- and δ^{18}O-values of calcite due to re-equilibration with organic fluids has already been described by Bechtel and Püttmann (1991).

The preceding analysis informs us essentially on the origin of the fluid phase involved in vein formation. We could not detect any evidence for intervention of an external fluid of either meteoric, hydrothermal or "basement" origin. Accordingly, we conclude that the

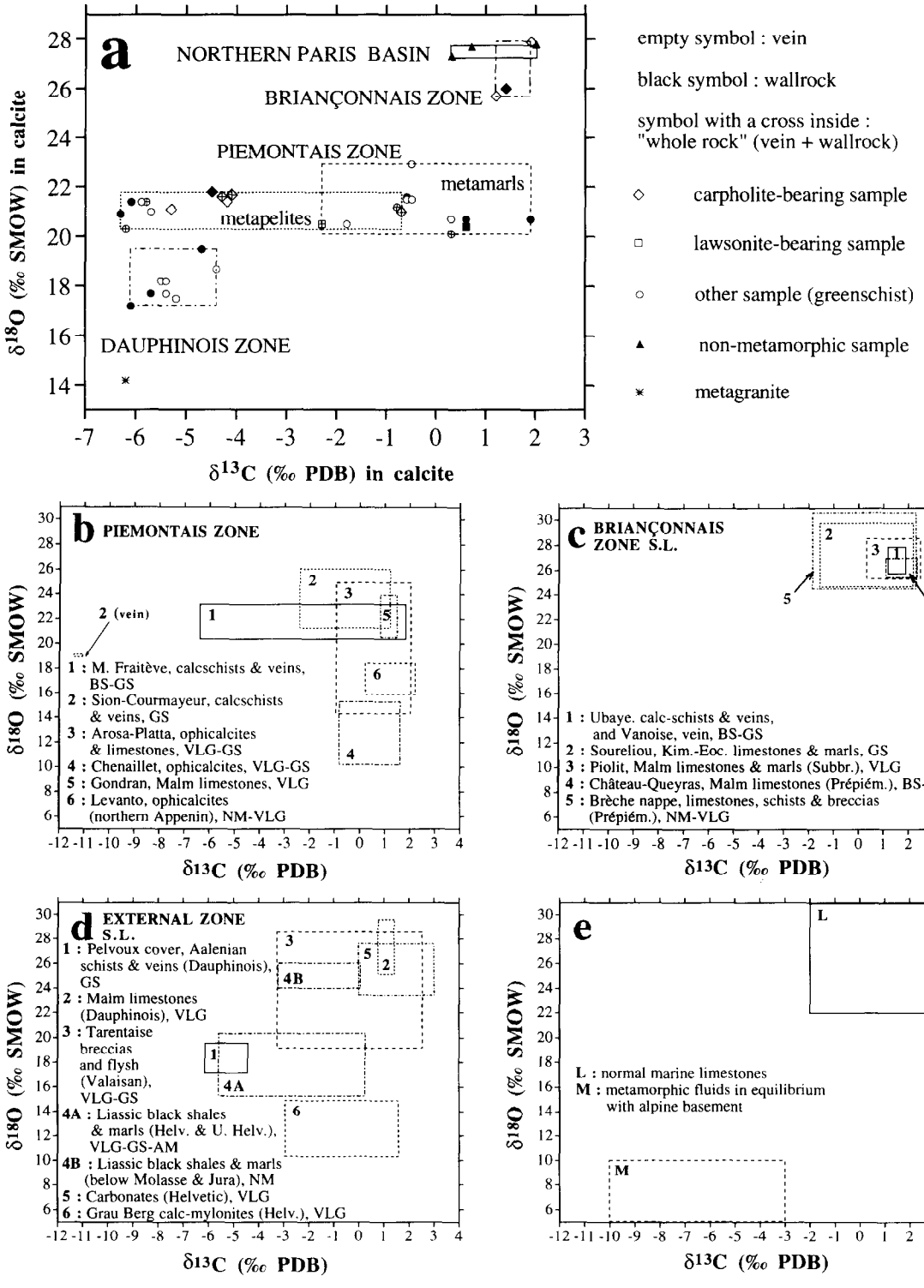
a
NORTHERN PARIS BASIN
BRIANÇONNAIS ZONE
PIEMONTAIS ZONE
metamarls
metapelites
DAUPHINOIS ZONE
δ18O (‰ SMOW) in calcite
δ13C (‰ PDB) in calcite
empty symbol : vein
black symbol : wallrock
symbol with a cross inside : "whole rock" (vein + wallrock)
carpholite-bearing sample
lawsonite-bearing sample
other sample (greenschist)
non-metamorphic sample
metagranite
b PIEMONTAIS ZONE
2 (vein)
1 : M. Fraitève, calcschists & veins, BS-GS
2 : Sion-Courmayeur, calcschists & veins, GS
3 : Arosa-Platta, ophicalcites & limestones, VLG-GS
4 : Chenaillet, ophicalcites, VLG-GS
5 : Gondran, Malm limestones, VLG
6 : Levanto, ophicalcites (northern Appenin), NM-VLG
c BRIANÇONNAIS ZONE S.L.
1 : Ubaye, calc-schists & veins, and Vanoise, vein, BS-GS
2 : Soureliou, Kim.-Eoc. limestones & marls, GS
3 : Piolit, Malm limestones & marls (Subbr.), VLG
4 : Château-Queyras, Malm limestones (Prépiém.), BS-GS
5 : Brèche nappe, limestones, schists & breccias (Prépiém.), NM-VLG
d EXTERNAL ZONE S.L.
1 : Pelvoux cover, Aalenian schists & veins (Dauphinois), GS
2 : Malm limestones (Dauphinois), VLG
3 : Tarentaise breccias and flysh (Valaisan), VLG-GS
4A : Liassic black shales & marls (Helv. & U. Helv.), VLG-GS-AM
4B : Liassic black shales & marls (below Molasse & Jura), NM
5 : Carbonates (Helvetic), VLG
6 : Grau Berg calc-mylonites (Helv.), VLG
e
L : normal marine limestones
M : metamorphic fluids in equilibrium with alpine basement

involved fluid phase originated in the rocks themselves (formation waters and "metamorphic" water linked to dehydration reactions), which acted as an isotopic reservoir. A local increased concentration of carbon in the fluid phase is suggested by low calcite $\delta^{13}C$-values in the Piémontais metapelites and the Dauphinois black shales.

4.4. H/O systematics in whole rocks, minerals and fluids

δD vs. $\delta^{18}O$ of analysed minerals and whole rocks are represented in Fig. 6. Hydrated minerals as well as whole rocks are characterized by high $\delta^{18}O$ and high δD, with whole-rock values tightly clustered around $-60‰$ δD and comprised between $+15$ and $+25‰$ $\delta^{18}O$, regardless of metamorphic grade and tectonic unit. A comparison with the isotopic composition of hydrated minerals from basement (Fig. 6a) and cover rocks (Fig. 6b) of the Western and Central Alps calls for the following remarks:

(1) Fe–Mg-carpholites show the most D-enriched values, with δD between -55 and $-40‰$; these values lie well within the field — or rather at the upper limit — of δD previously measured in hydrated minerals from Alpine basement and cover rocks. Fe–Mg-carpholites also show the most ^{18}O-enriched values, with $\delta^{18}O$ between $+17.5$ and $+25‰$; these values are those expected for minerals in calcite-dominated rocks (see Section 3.3).

(2) $\delta D/\delta^{18}O$-values of analyzed minerals and whole rocks lie in the field of carbonate cover rocks (e.g., 1, 4, 5 in Fig. 6b). Moreover, neither δD nor $\delta^{18}O$ depletion is evident in our samples, as indicated by their grouping in the "upper right corner" of an "Alpine cover rock box". A D depletion (vertical trend), has been observed in many areas of the Alps (e.g., 1 and 4 in Fig. 6a; 1, 2 and 4 in Fig. 6b), generally interpreted as the result of interaction with an external fluid, either an ancient or modern Alpine high-altitude meteoric water (see AMW in Fig. 6b, cf. Kullin and Schmassmann, 1991), or an organic water (Sheppard, 1986). A $\delta^{18}O$ depletion (horizontal trend) would indicate an interaction with a fluid in equilibrium, either with basement rocks (see Fig. 7a), or with quartz-rich cover rocks (see Fig. 7b). Interaction with any of the preceding types of fluids can be ruled out in the studied areas.

Calculated composition of fluids in equilibrium with the analyzed minerals and whole rocks are represented in Fig. 7. Trends can be summarized as follows:

(1) $\delta D/\delta^{18}O$ composition of a fluid in equilibrium with Fe–Mg-carpholite during HP metamorphism has been estimated using fractionation factors between quartz–water, quartz–hornblende and hornblende–water from Clayton et al. (1972), Bottinga and Javoy (1973) and Graham et al. (1984), respectively, at 350°C. Calculated $\delta^{18}O/\delta D$ of HP fluids are $\sim -25‰/+25‰$, which is not significantly different with regard to LP fluids (in equilibrium with chlorite and whole rocks), calculated at $\sim -25‰/+18‰$. Calculated $\delta^{18}O$ composition of waters in equilibrium with calcite lies in the same range, between $+14$ and $+22‰$ SMOW, using O'Neil et al. (1969) fractionation factor at 350°C.

(2) Isotopic fluid compositions lie well within the field of metamorphic waters in O and H equilibrium with Alpine cover rocks. In fact, they plot within the least depleted ("upper right") corner of the "metamorphic water box". This observation again indicates that the studied rocks have not suffered any detectable interaction with an external fluid.

Fig. 5. Carbon and oxygen isotopic compositions of calcites from Western and Central Alps.

a. Systematics in the studied samples.

b. Data from the Piémontais zone, after: 1 = this study; 2 = Burkhard and Kerrich (1988); 3 = Weissert and Bernoulli (1984); 4–6 = Lemoine et al. (1983).

c. Data from the Briançonnais zone, after: 1 = this study; 2 = M. Bourbon (in Brosse, 1982); 3 = Brosse (1982) and Lemoine et al. (1983); 4 = Lemoine et al. (1983); 5 = Brosse (1982).

d. Data from the External zone, after: 1 = this study; 2 = Lemoine et al. (1983); 3 = Gély et al. (1989); 4 = Hoefs and Frey (1976); 5, 6 = Burkhard et al. (1992).

e. *L* = estimated, after Keith and Weber (1964); *M* = estimated by Burkhard et al. (1992).

"Boxes" are drawn after extreme values, except 5 in (d), drawn after mean and 2σ-values, and *L* and *M*, estimated. In (b)–(d), Alpine metamorphic grade(s) are reported as follows: *BS* = blueschist; *AM* = amphibolite; *GS* = greenschist; *VLG* = very low grade; *NM* = non-metamorphic.

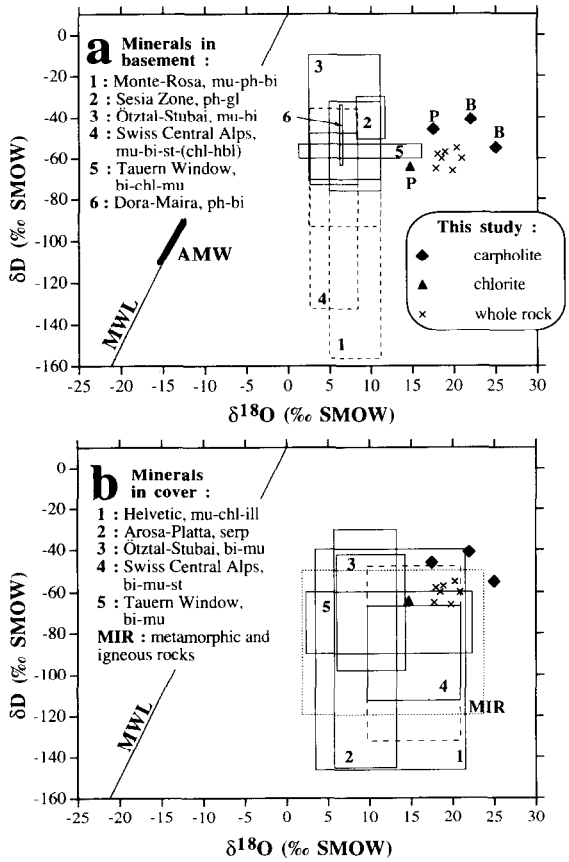

Fig. 6. Oxygen and hydrogen isotopic compositions of minerals from Western and Central Alps.

a. Data from basement rocks, after: 1 = Frey et al. (1976); 2 = Desmons and O'Neil (1978); 3 = Hoernes and Friedrichsen (1978); 4 = Hoernes and Friedrichsen (1980); 5 = Hoernes and Friedrichsen (1974) and Friedrichsen and Morteani (1979); 6 = Sharp et al. (1993).

b. Data from cover rocks, after: 1 = Hunziker et al. (1986) and Burkhard et al. (1992); 2 = Früh-Green et al. (1990); 3 = Hoernes and Friedrichsen (1978); 4 = Hoernes and Friedrichsen (1980); 5 = Hoernes and Friedrichsen (1974) and Friedrichsen and Morteani (1979); *MIR* = Hoefs (1987). "Boxes" are drawn after extreme values. Abbreviations: *bi* = biotite; *chl* = chlorite; *gl* = glaucophane; *hbl* = hornblende; *ill* = illite; *mu* = muscovite; *ph* = phengite; *st* = staurolite; *serp* = serpentine; *MWL* = Meteoric Water Line; *B* = Briançonnais zone; *P* = Piémontais zone.

Conclusions that can be drawn from $\delta D/\delta^{18}O$ systematics are the following: (1) in the studied areas, we can rule out the intervention of external fluids, such as meteoric waters, organic waters (?), fluids in equilibrium with basement or quartz-rich cover rocks; a similar conclusion on the range of fluid exchange during

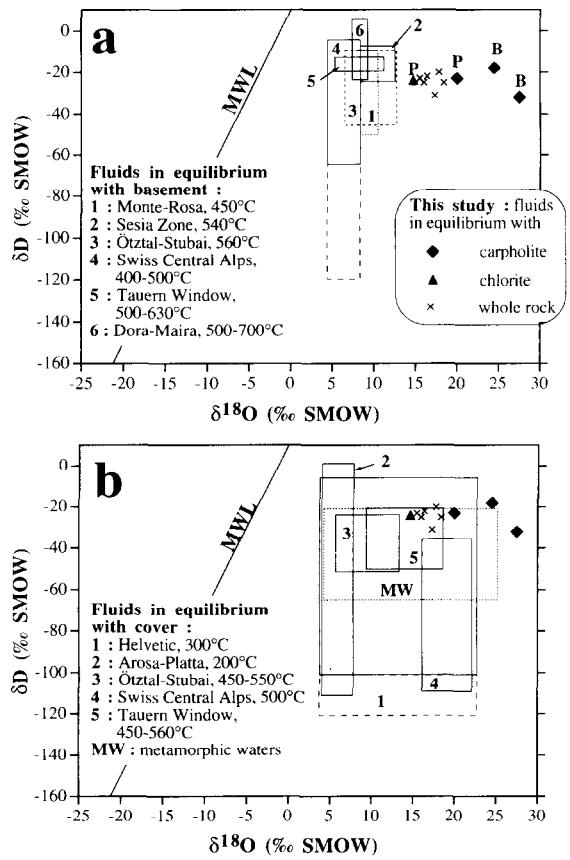

Fig. 7. Calculated H- and O-isotopic compositions of fluids in Western and Central Alps. Data from basement rocks (a) and from cover rocks (b): same sources as in Fig. 6. $\delta^{18}O$ fluid composition is calculated using quartz–water fractionation factors from Clayton et al. (1972) and Bottinga and Javoy (1973); muscovite–water and biotite–water fractionation factors (Bottinga and Javoy, 1973) are used for Dora–Maira (6 in Fig. 6a), and data of Wenner and Taylor (1971) for Arosa–Platta (2 in Fig. 6b). δD fluid composition is calculated using mineral–water fractionation factors from Suzuoki and Epstein (1976) for biotite, muscovite and hornblende, and from C.M. Graham (in Kyser, 1987, p.50) for chlorite; data of Wenner and Taylor (1973) are used for Arosa–Platta (2 in Fig. 6b). For data of this study, isotopic composition of fluids: (1) in equilibrium with chlorite, is calculated after chlorite–water data from Wenner and Taylor (1971) for O and from C.M. Graham (in Kyser, 1987, p.50) for H, at 300°C; (2) in equilibrium with carpholite, is estimated after quartz–water (Clayton et al., 1972) and quartz–hornblende (Bottinga and Javoy, 1973) data for O, and after hornblende–water data (Graham et al., 1984) for H, at 350°C; and (3) in equilibrium with whole rock, is estimated as follows: $\delta^{18}O_{(fluid)} = \delta^{18}O_{(w.r.)} - 2.5$ (‰ SMOW) and $\delta D_{(fluid)} = \delta D_{(w.r.)} + 35$ (‰ PDB).

Table 3
Major-element compositions of Piémontais and northern Paris Basin samples

	Piémontais zone													
	preserved carpholite-bearing samples						retrogressed carpholite-bearing samples							
	Sest911f[a]	± σ	Sest911m[a]	± σ	Sest911g[a]	± σ	Sest911wr[b]	CBas912f[a]	± σ	CBas912m[a]	± σ	CBas912g[a]	± σ	CBas912 wr[b]
SiO_2	59.23	0.74	64.69	0.46	76.43	0.88	69.07	58.58	0.46	68.56	0.81	78.87	3.76	70.54
Al_2O_3	20.77	0.98	17.05	0.20	11.04	0.95	15.03	19.03	0.77	14.96	0.84	8.80	0.69	13.21
Fe_2O_3	1.55	0.25	1.52	0.43	0.71	0.08	1.13	2.59	0.27	2.07	0.13	1.83	0.49	2.11
FeO	5.52	0.09	4.91	0.05	3.34	0.08	4.29	4.54	0.17	3.74	0.11	2.05	0.10	3.16
MnO	0.33	0.00	0.31	0.01	0.42	0.02	0.37	0.70	0.01	0.46	0.01	0.36	0.02	0.49
MgO	0.42	0.00	0.36	0.01	0.25	0.00	0.32	2.77	0.07	2.19	0.08	1.37	0.13	1.97
CaO	0.91	0.06	0.88	0.02	1.70	0.42	1.28	0.68	0.03	0.68	0.09	0.74	0.36	0.71
Na_2O	1.25	0.18	1.03	0.22	0.36	0.01	0.75	0.98	0.08	0.70	0.03	0.34	0.04	0.61
K_2O	3.18	0.08	2.73	0.11	1.44	0.08	2.21	3.22	0.22	2.34	0.12	1.22	0.18	2.06
TiO_2	0.76	0.05	0.50	0.08	0.31	0.02	0.47	0.75	0.03	0.53	0.01	0.28	0.04	0.48
P_2O_5	0.16	0.01	0.19	0.05	0.16	0.06	0.17	0.13	0.02	0.10	0.01	0.11	0.02	0.11
H_2O tot	4.65	0.04	3.93	0.40	2.48	0.31	3.40	4.74	0.22	3.54	0.16	2.38	0.29	3.34
LOI	5.76	0.53	4.78	0.09	4.44	0.36	4.85	5.02	0.16	4.00	0.12	2.83	0.19	3.74
Sum	99.83	0.77	98.92	0.35	100.58	1.25	99.95	99.01	0.99	100.33	0.38	98.79	2.06	99.18

	Piémontais zone (cont.)							Northern Paris Basin		
	carpholite-free samples									
	Frai911f[a]	± σ	Frai911m[a]	± σ	Frai911g[a]	± σ	Frai911wr[b]	Arg1	Arg2	Arg4
SiO_2	51.03	0.94	54.96	1.37	58.34	2.66	54.83	60.18	67.65	49.98
Al_2O_3	16.06	0.22	10.83	0.67	4.13	0.80	10.15	10.03	6.01	16.67
Fe_2O_3	2.48	0.39	1.99	0.02	0.97	0.14	1.78	3.54	5.36	3.78
FeO	4.45	0.05	3.43	0.10	1.65	0.27	3.12	1.19	1.48	1.10
MnO	0.28	0.02	0.23	0.01	0.17	0.02	0.23	0.00	0.00	0.00
MgO	2.85	0.12	2.18	0.06	1.52	0.14	2.17	1.48	1.04	1.48
CaO	7.20	0.20	10.83	0.24	16.55	0.77	11.71	8.47	6.23	7.70
Na_2O	1.01	0.02	0.76	0.02	0.42	0.04	0.72	0.16	0.15	0.27
K_2O	2.93	0.11	1.81	0.07	0.52	0.14	1.72	2.27	2.44	2.80
TiO_2	0.71	0.07	0.42	0.04	0.13	0.03	0.41	0.46	0.25	0.80
P_2O_5	0.12	0.02	0.08	0.01	0.03	0.01	0.08	0.91	1.15	0.06
H_2O tot	4.37	0.51	3.13	0.16	0.81	0.14	2.69	6.40	4.66	8.21
LOI	10.03	0.07	12.26	0.09	15.39	0.83	12.65	13.93	8.76	14.77
Sum	99.13	0.57	99.78	0.74	99.82	0.57	99.56	102.62	100.52	99.41

[a]Mean of 4 (Sest) or 3 (Frai and CBas) analyses. See Section 3.1 for sampling procedure.
[b]Whole-rock composition calculated from f, m and g fractions composition and corresponding weight.

Table 4
Trace-element compositions of the studied samples

Element (ppm)	Li	Be	Sc	V	Rb	Sr	Y	Zr	Nb	Mo	Cs	Ba	Hf	Ta	Tl	Pb	Bi	Th	U
Piémontais zone (preserved carpholite-bearing samples):																			
Fre6	36.1	1.23	16.1	123	65.3	98.6	15.8	58.3	15.9	1.84	4.63	362	1.71	2.82	0.36	20.1	0.56	13.5	2.08
Sest911f[a]	72.6	3.05	20.1	167	164	116	21.7	109	19.3	3.68	9.14	353	3.11	1.70	0.99	30.7	0.49	12.8	2.58
± σ	2.20	0.37	0.28	1.18	1.65	0.73	2.88	5.47	0.43	0.13	0.13	3.15	0.15	0.06	0.03	5.24	0.02	0.13	0.06
Sest911m[a]	60.4	2.64	16.7	138	138	98.8	15.2	71.6	14.0	3.06	7.54	289	2.03	1.50	0.86	23.9	0.36	9.12	1.78
± σ	1.30	0.09	0.18	2.31	2.07	0.97	4.22	12.65	0.24	0.19	0.11	4.24	0.47	0.08	0.02	1.83	0.01	0.36	0.13
Sest911g[a]	33.4	1.12	10.2	77.6	78.3	82.7	12.7	29.4	6.37	1.81	4.19	153	0.90	1.28	0.44	20.9	0.16	4.49	0.86
± σ	0.29	0.21	0.37	2.59	3.35	7.17	1.20	2.96	0.30	0.11	0.16	5.31	0.10	0.15	0.04	5.74	0.03	0.18	0.06
Piémontais zone (retrogressed carpholite-bearing samples):																			
CBas912f[a]	89.2	3.00	19.2	161	145	96.9	14.2	82.0	16.5	1.17	8.78	411	2.37	1.84	0.88	21.4	0.50	10.6	1.93
± σ	5.16	0.06	0.31	4.73	5.38	1.80	0.99	5.49	0.17	0.16	0.20	12.2	0.08	0.15	0.03	4.29	0.02	0.34	0.08
CBas912m[a]	71.9	2.06	15.0	122	113	80.5	9.48	46.6	11.7	0.90	6.80	315	1.36	1.47	0.66	17.5	0.36	7.59	1.26
± σ	2.41	0.10	0.16	4.56	2.39	4.97	0.84	4.18	0.49	0.05	0.06	7.46	0.14	0.13	0.01	2.49	0.02	0.16	0.05
CBas912g[a]	40.7	1.13	7.89	63.0	57.9	58.9	7.52	25.1	5.57	1.00	3.39	158	0.72	1.34	0.34	14.0	0.16	4.05	0.69
± σ	7.99	0.12	2.04	15.8	14.5	8.92	0.92	4.16	1.59	0.15	0.84	39.5	0.11	0.16	0.09	2.99	0.03	1.18	0.17
Piémontais zone (carpholite-free samples):																			
Fre8	32.4	0.11	5.20	16.9	4.63	682	25.4	10.0	2.52	0.16	0.26	15.9	0.23	2.18	0.03	4.34	0.10	1.07	0.33
Fre15	44.1	0.32	9.15	33.8	23.5	800	48.1	7.87	3.07	2.21	1.62	45.5	0.27	1.61	0.13	18.1	0.16	1.71	0.26
Fre16s	25.1	0.59	6.41	52.4	57.4	1019	16.2	13.5	4.86	3.11	4.06	110	0.38	1.10	0.31	10.1	0.16	4.12	0.46
Fre16m	59.7	1.46	13.6	113	118	499	18.5	41.6	13.2	2.88	8.21	242	1.28	1.78	0.63	14.3	0.34	8.69	1.30
Fre22	26.9	1.13	9.80	58.6	80.4	467	12.0	29.8	9.12	0.42	4.68	193	0.87	3.62	0.41	7.53	0.14	4.42	0.84
Fre1CH	1.17	0.00	4.50	2.21	0.91	434	5.83	4.34	2.44	0.08	0.08	3.68	0.12	2.25	0.00	4.94	0.06	0.47	0.19
Frai911f[a]	64.6	2.36	16.6	127	130	216	18.3	97.1	13.8	0.61	8.12	381	2.81	1.49	0.69	18.3	0.42	10.4	2.03
± σ	0.40	0.13	0.16	3.25	5.84	8.15	1.45	8.40	0.74	0.07	0.45	13.7	0.20	0.05	0.03	2.52	0.01	0.56	0.17
Frai911m[a]	49.0	1.54	12.3	88.7	87.3	319	14.9	59.2	8.80	0.56	5.29	265	1.72	1.29	0.45	13.7	0.29	6.79	1.30
± σ	1.08	0.40	0.17	1.11	0.31	10.7	0.13	1.42	0.17	0.01	0.07	1.91	0.05	0.13	0.03	2.84	0.02	0.13	0.02
Frai911g[a]	15.2	0.36	5.06	26.4	25.2	466	9.42	16.8	2.73	0.43	1.51	73.1	0.48	0.81	0.13	11.9	0.14	2.17	0.51
± σ	3.81	0.27	0.74	7.48	7.70	36.5	1.25	4.28	0.68	0.12	0.46	22.0	0.07	0.05	0.05	2.39	0.01	0.50	0.09
Northern Paris Basin:																			
Arg1	50.9	2.64	12.0	98.2	143	315	21.6	111	13.7	1.04	11.2	243	3.16	0.93	0.61	14.2	0.27	9.21	3.31
Arg2	19.0	2.23	6.25	50.4	99.2	143	24.3	68.1	6.00	0.48	3.69	134	1.78	0.37	0.24	10.7	0.12	5.07	2.38
Arg4	165	2.58	15.7	163	136	350	20.3	154	22.4	0.35	11.9	358	4.44	1.53	0.73	31.4	0.48	13.1	2.78
Briançonnais zone:																			
Van	48.0	0.00	4.32	8.60	5.30	502	23.7	2.26	1.04	0.10	0.30	40.5	0.08	0.98	0.07	2.01	0.10	0.40	0.19
Ub873s	4.17	0.05	2.00	7.42	4.56	947	19.7	5.24	1.53	0.05	0.35	57.3	0.15	0.88	0.03	5.90	0.07	0.78	0.22
Ub873m	46.0	0.58	6.11	51.4	39.5	1389	19.0	40.8	7.78	0.14	2.92	324	1.19	1.16	0.21	11.1	0.30	6.39	1.83
Dauphinois zone:																			
Vent4s	95.0	0.19	2.32	10.3	9.09	283	10.4	2.36	0.99	0.26	0.60	15.2	0.13	0.47	0.00	11.6	0.10	0.98	0.15
Vent4m	303	4.05	23.8	243	174	405	12.4	0.00	27.1	1.33	12.6	392	3.67	2.32	0.95	22.1	0.58	19.0	3.06
Vilas	106	0.08	3.82	32.0	2.66	101	7.80	2.83	1.29	0.17	0.18	5.31	0.07	0.47	0.00	10.1	0.05	0.69	0.09
Vilam	307	1.36	14.2	179	72.6	137	9.49	68.1	21.8	1.37	4.67	160	1.83	1.47	0.41	14.3	0.27	10.9	1.63
Vila16	858	0.44	4.56	16.2	0.28	118	16.6	0.24	1.07	0.05	0.07	0.91	0.02	1.46	0.00	4.79	0.04	0.33	0.04
Laz2s	18.8	0.03	3.28	2.49	1.94	74.0	14.7	1.9	2.39	0.19	0.22	4.02	0.09	3.16	0.00	6.02	0.02	0.71	0.05
Laz2m	184	3.39	16.6	193	137	291	13.8	59.8	23.4	4.00	16.5	310	1.47	3.21	0.87	22.4	0.29	11.8	1.61
Jar4s	4.28	0.00	2.22	3.79	2.62	172	15.3	1.5	1.13	0.11	0.25	4.47	0.08	1.45	0.00	263	0.28	0.36	0.03
Jar4m	157	4.38	29.8	312	255	405	12.7	147	51.9	3.03	21.7	604	4.02	3.24	1.55	27.6	0.78	26.4	3.74
Jarsoc	17.4	2.52	3.33	16.4	138	205	7.34	30.8	13.5	0.25	6.09	202	0.94	2.22	1.79	25.5	0.10	21.0	1.50

[a]Mean of 4 (Sest) or 3 (CBas and Frai) analyses. See Section 3.1 for sampling procedures.

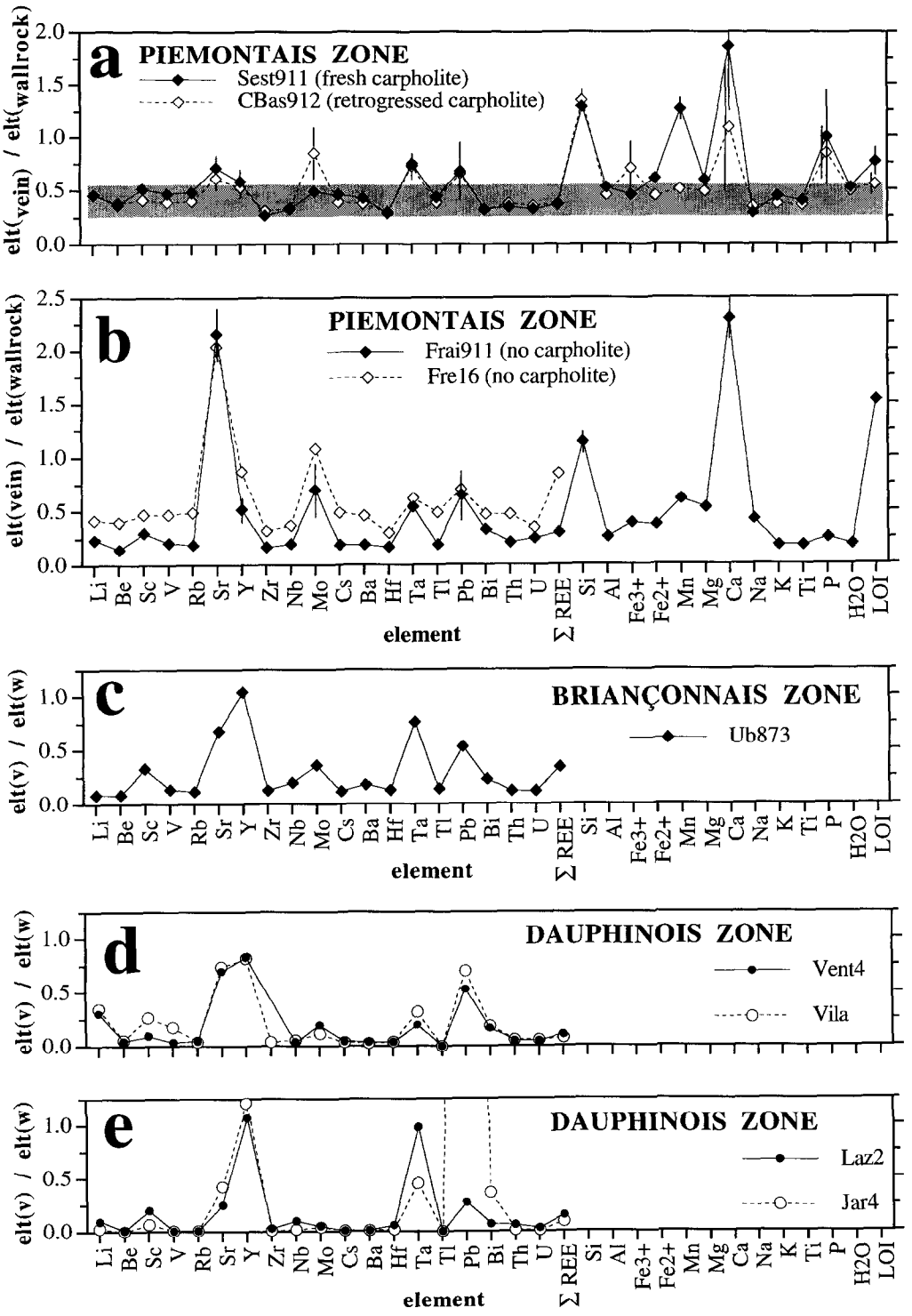

Fig. 8. Ratio plot for various trace and major elements in the vein relative to the wallrock. Elements within the shaded grey area in (a) are considered as immobile during vein formation. Vertical bars in (a) and (b) represent $\pm 1\sigma$ for elements considered as enriched in the vein.

Alpine metamorphism has been drawn by Hoernes and Friedrichsen (1980); (2) veins formed from an "internal fluid" in O- and H- isotopic equilibrium with carbonate-rich cover rocks; and (3) the isotopic composition of this internal fluid seems to have been essentially the same during the prograde and the retrograde metamorphic evolution.

4.5. Major- and trace-element systematics

Major- and trace-element compositions of the studied samples are presented in Table 3 and Table 4, respectively.

In order to test for element mobility between wallrocks and veins, we plotted the different trace and major elements in various concentration ratio diagrams (element in vein/element in wallrock, Fig. 8). In such diagrams (e.g., Gresens, 1967; Grant, 1986), elements which plot at similar *Y*-values display the same behaviour during the transformation of the rock. In particular, assuming volume and mass conservation during element transfer, elements which plot near the *Y*-axis unity line are immobile (same concentration in the vein and in the wallrock). Confrontation with our results calls for the following remarks:

(1) In all the studied zones, a large set of analysed elements (Li, Be, Sc, V, Rb, Zr, Nb, Cs, Ba, Hf, Tl, Bi, Th, U, ΣREE, Al, Fe, Mg, Na, K, Ti, H_2O) plot invariably at low and constant *Y*-values. This "bottom line" *Y*-value is shaded in grey in Fig. 8a. Although the absolute *Y*-value is different in each sample, the same trends are present in all samples. All these elements apparently behave in the same manner during vein formation. Two interpretations are possible: (a) the quoted elements are all immobile, i.e. they are not precipitated in the vein-forming minerals; consequently, vein formation is a mechanism where volume and/or mass are not preserved; and (b) alternatively the quoted elements are all mobile, and enriched in the wallrock with respect to the vein, assuming an isovolume and isodensity mechanism of vein formation. The first hypothesis seems to be more convincing, in an opening/shearing context of vein formation, accompanied by local volume increase in the vein, and volume loss in the wallrock. Moreover, many of the above quoted elements (e.g., Zr, Hf, Th, REE, Ti) are classically considered to be inert and not susceptible to mobilization during low-grade metamorphism (e.g., Floyd and Winchester, 1978; Petersen, 1983; Zielinski, 1985; Bebout et al., 1993). Therefore, we consider in the following that elements, which plot clearly above the "bottom line" defined by a majority of immobile elements, are enriched in the veins with respect to their wallrock.

(2) In the Piémontais zone (Fig. 8a and b), veins are invariably enriched in Si, Ca and Sr — related to massive quartz (Si) and calcite (Ca, Sr) crystallization in veins, and also probably to aragonite crystallization (during early HP metamorphism), as still recognized in the Vanoise area (Gillet and Goffé, 1988) and in the Betic Cordilleras, Spain (Goffé et al., 1989). Part of Ca is also contained in apatite, together with P (Fig. 8a). In the preserved carpholite-bearing sample (plain symbol in Fig. 8a), the intriguing strong Mn enrichment is probably accommodated in Fe–Mg-carpholite, which can contain up to 1% MnO, and/or in chlorite (breakdown product of Fe–Mg-carpholite). The trace elements Pb, Ta and Y, enriched in veins with respect to their wallrocks in all the studied samples, can be explained as follows (cf. Wedepohl, 1978): (a) Pb can be contained in carbonates, as already observed in Fe–Mg-carpholite-bearing schists from the Betic Cordilleras, but also in phosphate; the very high Pb content in vein Jar4 should be, either an analytical error or related to accessory galena crystallization, as observed in some veins from the Vanoise area; (b) Ta is probably accommodated in rutile and/or another oxide; and (3) Y enters in solid solution in apatite.

From this preliminary analysis it results that, in all the studied zones, few elements (Sr, Y, Ta, Pb, Si, Ca, P) are clearly enriched in the veins with respect to their wallrock — related to the crystallization of quartz and carbonates, together with phosphate and oxide — whereas a majority of elements are immobile and have been passively enriched in wallrock during the vein formation. This observation is in agreement with a small-scale (ten centimetres to a few metres) migration of selected elements from wallrock to vein (compare Burkhard and Kerrich, 1988; Gray et al., 1991). This element transfer leading to vein formation could be accounted for by ionic diffusion processes.

4.6. Rare-earth element systematics

REE compositions of the studied samples are presented in Table 5. Chondrite-normalized REE abundances for selected samples are represented in Fig. 9:

Table 5
REE compositions of the studied samples

Element (ppm)	La	Ce	Pr	Nd	Sm	Eu	Gd	Tb	Dy	Ho	Er	Tm	Yb	Lu	Sum REE
Piémontais zone (preserved carpholite-bearing samples):															
Fre6	27.3	57.3	6.18	24.0	4.11	0.84	3.69	0.50	3.29	0.61	1.73	0.26	1.59	0.22	132
Sest911f[a]	39.9	84.1	9.30	36.4	6.99	1.49	6.13	0.78	4.51	0.83	2.35	0.35	2.33	0.35	196
± σ	0.55	0.89	0.12	0.36	0.12	0.05	0.39	0.05	0.49	0.10	0.33	0.04	0.19	0.03	3.73
Sest911m[a]	26.8	57.6	6.47	26.2	5.32	1.18	4.68	0.56	3.31	0.59	1.63	0.24	1.58	0.24	136
± σ	4.45	8.05	0.78	2.03	0.31	0.09	0.62	0.11	0.65	0.16	0.43	0.06	0.40	0.06	18.2
Sest911g[a]	12.6	27.9	3.26	13.7	3.60	1.19	3.79	0.49	2.78	0.47	1.26	0.18	1.07	0.16	72.5
± σ	0.39	0.52	0.07	0.38	0.16	0.12	0.24	0.02	0.22	0.04	0.09	0.02	0.07	0.00	2.34
Piémontais zone (retrogressed carpholite-bearing samples):															
CBas912f[a]	34.3	74.0	7.96	30.9	5.63	1.09	4.24	0.51	2.99	0.55	1.64	0.25	1.84	0.27	166
± σ	2.28	4.27	0.44	1.98	0.41	0.11	0.36	0.02	0.26	0.04	0.09	0.02	0.15	0.02	10.4
CBas912m[a]	21.5	46.2	5.04	20.0	3.73	0.75	2.84	0.35	2.07	0.40	1.13	0.17	1.20	0.18	106
± σ	1.61	3.12	0.29	0.93	0.24	0.04	0.10	0.01	0.09	0.02	0.10	0.01	0.12	0.02	6.71
CBas912g[a]	11.3	25.8	2.93	12.4	3.03	0.66	2.54	0.30	1.71	0.30	0.80	0.12	0.71	0.10	62.7
± σ	2.87	5.64	0.59	2.35	0.23	0.05	0.23	0.02	0.13	0.03	0.08	0.02	0.12	0.02	12.4
Piémontais zone (carpholite-free samples):															
Fre8	8.96	16.1	2.71	15.3	6.69	2.17	7.48	0.99	5.31	0.84	2.06	0.25	1.43	0.19	70.5
Fre15	20.0	51.0	7.23	33.9	10.3	3.91	11.7	1.63	9.29	1.52	3.81	0.45	2.45	0.31	158
Fre16s	15.2	31.0	3.95	19.6	6.85	1.99	6.86	0.80	4.03	0.60	1.36	0.17	0.95	0.12	93.5
Fre16m	20.9	41.3	5.08	21.0	5.36	1.51	5.69	0.75	4.23	0.71	1.93	0.27	1.70	0.25	111
Fre22	13.4	27.9	3.54	15.3	3.47	0.86	3.42	0.45	2.68	0.49	1.26	0.19	1.22	0.17	74.4
Fre1CH	2.51	10.3	1.91	9.35	2.11	0.47	1.94	0.26	1.45	0.22	0.46	0.04	0.17	0.02	31.2
Frai911f[a]	33.5	67.2	7.70	30.1	5.40	1.04	4.53	0.60	3.72	0.71	2.12	0.32	2.16	0.33	159
± σ	1.82	2.84	0.38	0.94	0.22	0.04	0.31	0.06	0.25	0.06	0.22	0.04	0.23	0.03	7.42
Frai911m[a]	21.6	45.5	5.61	23.6	4.76	1.01	4.16	0.53	3.15	0.56	1.58	0.23	1.48	0.22	114
± σ	0.28	0.37	0.04	0.51	0.19	0.01	0.04	0.01	0.03	0.01	0.01	0.01	0.05	0.01	1.55
Frai911g[a]	6.29	15.0	2.35	12.3	3.58	0.96	3.28	0.40	2.16	0.34	0.82	0.11	0.64	0.09	48.3
± σ	0.28	0.37	0.04	0.51	0.19	0.01	0.04	0.01	0.03	0.01	0.01	0.01	0.05	0.01	1.55
Northern Paris Basin:															
Arg1	35.1	61.7	7.84	30.9	5.52	1.12	5.07	0.66	4.08	0.80	2.29	0.34	2.15	0.33	158
Arg2	31.2	54.5	7.21	29.5	5.65	1.26	5.41	0.69	4.04	0.78	2.15	0.29	1.77	0.26	145
Arg4	35.6	79.9	8.35	31.0	5.50	1.31	4.76	0.69	4.32	0.83	2.49	0.38	2.44	0.39	178
Briançonnais zone:															
Van	3.62	15.0	3.50	16.8	3.64	0.54	3.36	0.53	3.50	0.65	1.65	0.18	0.89	0.12	53.9
Ub873s	3.18	6.71	1.43	8.47	2.59	0.76	3.01	0.45	3.01	0.56	1.35	0.14	0.56	0.06	32.3
Ub873m	23.0	34.5	4.35	17.4	3.57	1.03	3.70	0.49	3.15	0.61	1.73	0.22	1.34	0.20	95.3
Dauphinois zone:															
Vent4s	2.20	6.88	1.09	6.32	3.31	4.01	3.02	0.39	2.12	0.34	0.89	0.11	0.63	0.08	31.4
Vent4m	64.1	133	14.1	50.8	8.01	0.92	5.47	0.66	3.75	0.68	2.02	0.34	2.27	0.34	286
Vilas	1.07	2.55	0.31	1.68	1.13	1.26	1.75	0.24	1.53	0.27	0.69	0.10	0.59	0.08	13.3
Vilam	33.0	72.9	7.32	27.5	5.60	1.01	4.71	0.54	2.72	0.44	1.19	0.18	1.18	0.18	158
Vila16	0.44	1.81	0.36	2.68	2.10	1.56	2.91	0.46	2.85	0.49	1.30	0.19	1.08	0.14	18.4
Laz2s	0.92	4.05	0.82	5.06	2.51	1.04	2.83	0.46	2.79	0.50	1.40	0.20	1.19	0.16	23.9
Laz2m	34.3	68.9	7.95	31.2	6.54	1.16	5.16	0.60	3.32	0.66	1.54	0.22	1.47	0.20	163
Jar4s	1.48	5.76	1.01	5.81	3.06	5.62	3.50	0.53	3.06	0.53	1.31	0.17	0.91	0.12	32.9
Jar4m	83.6	182	18.8	66.9	9.05	1.31	4.84	0.52	3.04	0.57	1.81	0.33	2.34	0.34	375
Jarsoc	45.2	85.3	9.24	32.7	4.96	0.75	3.40	0.36	1.73	0.26	0.65	0.09	0.53	0.07	185

[a]Mean of 4 (Sest) or 3 (CBas and Frai) analyses. See Section 3.1 for sampling procedures.

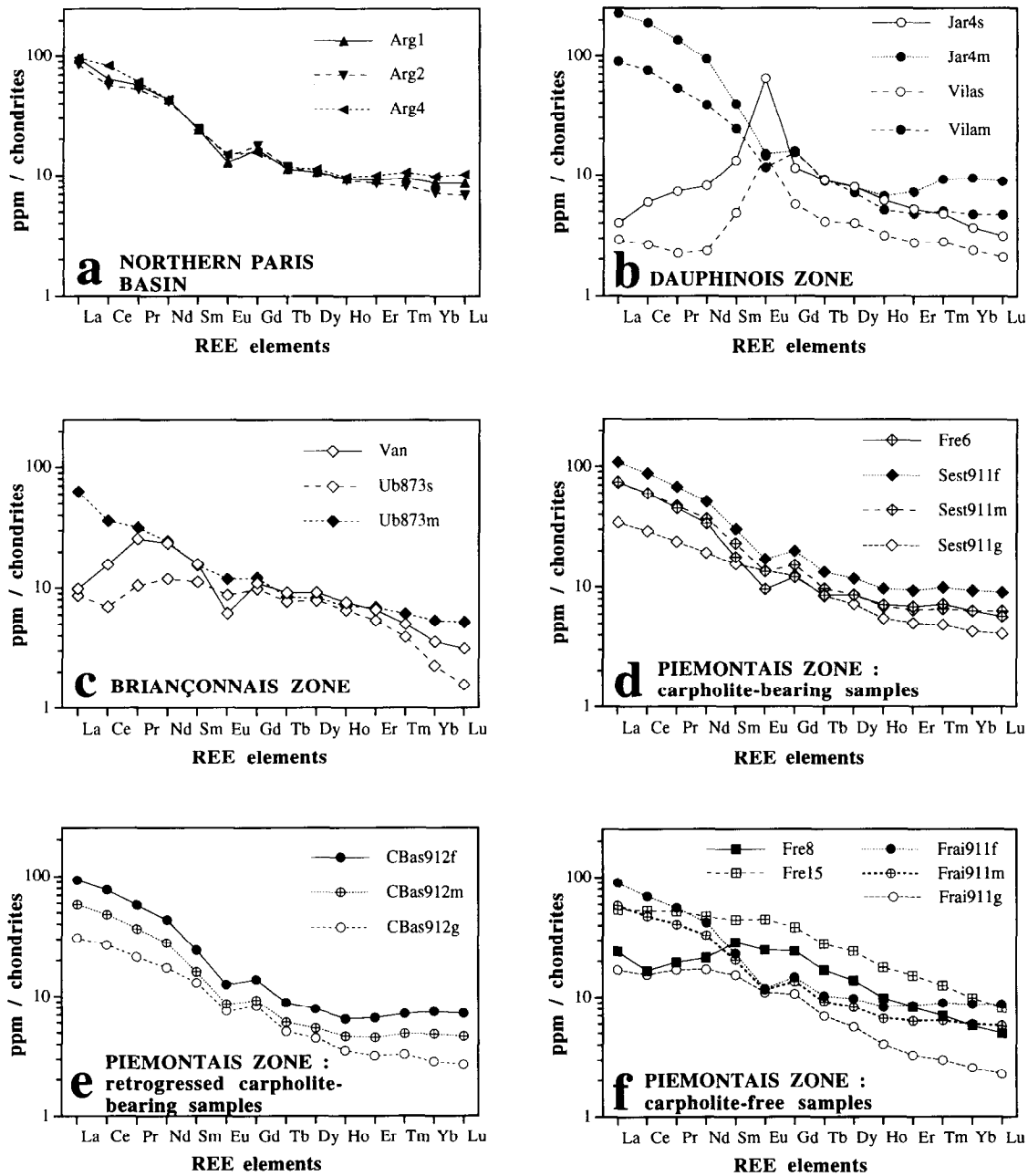

Fig. 9. Selected chondrite-normalized REE patterns in the studied samples. Same *symbols* as in Figs. 3 and 4.

(1) The patterns observed in non-metamorphic shales of the northern Paris Basin (Fig. 9a) are closely comparable to those of post-Archean Australian shales (PAAS, Taylor and McLennan, 1985). Such patterns are also characteristic of the schists in the Dauphinois zone (solid symbols in Fig. 9b), of the calc schist in the Briançonnais zone (sample Ub873m in Fig. 9c), and of most veins and wallrocks throughout the Piémontais zone (Fig. 9d–f). This observation confirms the northern Paris Basin shales as suitable protoliths

for the studied samples. Moreover, it appears that greenschist/blueschist-facies metamorphism has not significantly modified the REE "sedimentary pattern".

(2) Uncommon patterns are displayed by the veins of the Dauphinois zone (open symbols in Fig. 9b). Two features have to be explained: the low abundance of REE, especially of light REE (LREE), and the strong, positive Eu anomaly.

Observed low abundance of REE, known to be typical for carbonates (e.g., Haskin et al., 1966; Fleet, 1984), must certainly be related to the high calcite content of the Dauphinois veins; the same feature is also observed in the carbonate-rich segregation from Haute-Ubaye Valley (sample Ub873s in Fig. 9c).

Explanation of the positive Eu anomaly is more problematic. It must be linked to the presence of a "Eu-rich" phase. As plagioclase has not been detected in these veins, other candidates have to be sought. Tourmaline and epidote are minerals which are able to fractionate Eu (Alderton et al., 1980 and Nystrom, 1984, respectively), and which can be present in veins — although not detected so far in our samples. Another candidate is cookeite (Li-chlorite) and/or other phyllosilicates; positive Eu anomalies have previously been described in chlorite (Cullers et al., 1975) and biotite (Roaldset, 1975). Cookeite is present both in veins and in wallrock — although generally in lower amounts in the latter — so that an Eu anomaly should also be observed in the wallrock samples. Also interesting to be noted is the ability of calcite to fractionate Eu and other LREE: this behaviour has been described in a hydrothermal calcite from the Alps, suggesting Eu enrichment through a fluid phase (Lausch et al., 1974); the positive Eu anomalies also described in some metacarbonates of Colorado, U.S.A., has been attributed to the existence of Eu as Eu^{2+}, suggesting that the present pore fluids were reducing (Jarvis et al., 1975) — the presence of such a fluid might be inferred for the studied organic matter-rich Dauphinois schists.

REE systematics show thus different behaviour in the different studied zones, in particular: (1) in the Piémontais zone, veins display the same pattern as wallrocks, with a lower chondrite-normalized abundance of each REE in the vein; this behaviour is in agreement with a dilution effect as discussed in the context of trace elements; (2) in the Dauphinois zone, on the contrary, veins display very different patterns (in particular a strong positive Eu anomaly) compared to their wallrock; this difference could be related to the crystallization of an Eu-rich mineral phase, which might indicate "contamination" of calcite precipitated from an external fluid.

5. Final discussion and concluding remarks

For the studied areas of the Western Alps, information about the fluid phase involved in the vein formation are the following:

(1) *Fluid provenance*: Stable isotope data of the studied rocks do not show any evidence for interaction with an external fluid such as metamorphic fluids issued from Alpine basement or quartz-rich cover rocks, hydrothermal or meteoric waters. Accordingly, we conclude that the fluids involved in vein formation stem from the local rocks themselves, as formation water and metamorphic water produced in situ. General considerations (Fyfe et al., 1978; Marquer and Burkhard, 1992, p.1051 ff.) allow the total production of such waters to be estimated as between 1 and 4 vol% for greenschist-facies limestones and marls whereas up to 10% of metamorphic waters could be produced in pelites from the Dauphinois and Piémontais zones. Such fluids are in isotopic equilibrium with the "average local rock" which acts as a large isotopic reservoir for fluid production and vein formation ("rock-buffered system"). On a larger scale, however, part of these metamorphic fluids must leave the system — and will therefore interact with rocks elsewhere (e.g., Connolly and Thompson, 1989). Accordingly, the passage of small quantities of "far-travelled" metamorphic fluids is to be expected in any metamorphic terrain but these will be extremely difficult to document if their passage is sufficiently diffuse to permit a continuous equilibration with the rocks encountered along their pathways.

(2) *Chemical composition of vein-forming fluid phase*: The chemical composition of the fluid phase is poorly constrained by stable isotope data alone. Fluid inclusion studies in western Vanoise Fe–Mg-carpholite-bearing metasediments (Goffé, 1982; Goffé and Villey, 1984) show: (a) liquid inclusions composed mainly of H_2O with low content of eq wt% NaCl (5% max.); (b) liquid or gaseous heavy hydrocarbons (C_2 to C_{30}), immiscible with water, preserving therefore a high a_{H_2O}. Moreover, the presence of cookeite itself

implies high a_{H_2O} (cf. Vidal and Goffé, 1991). Cookeite is associated with Fe–Mg-carpholite in Vanoise (Goffé, 1977) and is also present in the Dauphinois zone (Jullien and Goffé, 1993). Petrological arguments thus indicate the presence of a H_2O-dominated fluid. Moreover, the fluid phase seems to have had approximately the same composition throughout the HP and subsequent LP metamorphic evolution.

(3) *Mechanisms of fluid flow and element transport*: In the considered metamorphic domains, fluid migration takes place within the main tectonic or lithologic units at different scales: (a) at hectometric scale, fluids in each zone are interpreted as essentially stationary or advected internally, in agreement with the isotopic "rock-buffered" behaviour (low fluid/rock ratios). Minor layer-parallel fluid flow cannot be ruled out, however; and (b) at small scale (cm to m), major- and trace-element systematics reveal selective element transfer from wallrock to adjacent vein, mainly achieved by ionic diffusion processes.

Fluid flow along and across the main tectonic contacts probably took place but is poorly documented. There may have been some local migration in the Dauphinois zone, where the metagranitic basement seems to have interacted with a "sedimentary fluid" from the overlying tectonic units on the scale of ~ 10 m. In the Western Alps, major tectonic contacts marked by metre- to decametre-thick evaporitic layers (e.g., Penninic Front; Fig. 1b), are probable fluid channels (Kerrich, 1986; McCaig, 1988), although not necessarily related to the vein formation.

Acknowledgements

This work was supported by a grant of the Fonds National Suisse (No. 20.27597.89). C.H. thanks particularly D. Pezderic (University of Saskatchewan, Canada) for introducing her to isotopic extraction techniques, N. Catel (ENS Paris, France) for performing wet chemical analyses, and J.C. Hunziker, D. Marquer, R. Oberhänsli, H.R. Pfeifer and Z.D. Sharp for helpful discussions. Y.F. Zheng is acknowledged for calculation of Fe–Mg-carpholite fractionation curves and for critical remarks. This paper benefited from the constructive reviews of N.T. Arndt, S. Hoernes and A. McCaig.

References

Agard, P. and Cuny, D., 1992. Fractales et structures fibreuses en domaine métamorphique. Lab. Géol., ENS (École Norm. Supér.), Paris, Intern. Rep. (unpublished).

Alderton, D.H.M., Pearce, J.A. and Potts, P.J., 1980. Rare earth element mobility during granite alteration: evidence from southwest England. Earth Planet. Sci. Lett., 49: 149–165.

Aprahamian, J., 1988. Cartographie du métamorphisme faible à très faible dans les Alpes françaises par l'utilisation de la cristallinité de l'illite. Geodyn. Acta, 2(1): 25–32.

Baker, A.J., 1990. Stable isotopic evidence for fluid–rock interactions in the Ivrea Zone, Italy. J. Petrol., 31(1): 243–260.

Baumgartner, L.P. and Rumble, D., 1988. Transport of stable isotopes, I: Development of a kinetic continuum theory for stable isotope transport. Contrib. Mineral. Petrol., 98: 417–430.

Bebout, G.E. and Barton, E.B., 1989. Fluid flow and metasomatism in a subduction zone hydrothermal system: Catalina schist terrane, California. Geology, 17: 976–980.

Bebout, G.E. and Barton, E.B., 1993. Metasomatism during subduction: products and possible paths in the Catalina Schists, California. In: J.L.R. Touret and A.B. Thompson (Guest-Editors), Fluid–Rock Interaction in the Deeper Continental Lithosphere. Chem. Geol., 108: 61–92 (special issue).

Bebout, G.E., Ryan, J.G., Leeman, W.P. and Bebout, A.E., 1993. Fractionation of trace element and stable isotope signatures during subduction-zone metamorphism. Eos (Trans. Am. Geophys. Union), 74: 331 (abstract).

Bechtel, A. and Püttmann, W., 1991. The origin of the Kupferschiefer-type mineralization in the Richelsdorf Hills, Germany, as deduced from stable isotope and organic geochemical studies. Chem. Geol., 91: 1–18.

Bottinga, Y. and Javoy, M., 1973. Comments on oxygen isotope geothermometry. Earth Planet. Sci. Lett., 20: 250–265.

Bouquillon, A., France-Lanord, C., Michard, A. and Tiercelin, J.J., 1990. Sedimentology and isotopic chemistry of the Bengal fan sediments: the denudation of the Himalaya. Proc. Ocean Drill. Prog. Sci. Results, 116: 43–58.

Bröcker, M., Kreuzer, H. Matthews, A. and Okrusch, M., 1993. $^{40}Ar/^{39}Ar$ and oxygen isotope studies of polymetamorphism from Tinos Island, Cycladic blueschist belt, Greece. J. Metam. Geol., 11: 223–240.

Brosse, E., 1982. Contribution à la minéralogie et à la géochimie des sédiments pélagiques profonds — Comparaison des "black-shales" du Crétacé dans l'Atlantique central nord et des dépôts du Malm et du Crétacé en Briançonnais. Thèse Doct. Ing., École Nationale Supérieure des Mines, Paris, 474 pp.

Burkhard, M. and Kerrich, R., 1988. Fluid regimes in the deformation of the Helvetic nappes, Switzerland, as inferred from stable isotope data. Contrib. Mineral. Petrol., 99: 416–429.

Burkhard, M. and Kerrich, R., 1990. Fluid rock interactions during thrusting of the Glarus nappe — evidence from geochemical and stable isotope data. Schweiz. Mineral. Petrogr. Mitt., 70: 77–82.

Burkhard, M., Kerrich, R., Maas, R. and Fyfe, W.S., 1992. Stable and Sr-isotope evidence for fluid advection during thrusting of the Glarus nappe (Swiss Alps). Contrib. Mineral. Petrol., 112: 293–311.

Caby, R., Kienast, J.R. and Saliot, P., 1978. Structure, métamorphisme et modèle d'évolution tectonique des Alpes occidentales. Rev. Géogr. Phys. Géol. Dyn., 4: 307–322.

Caron, J.M., 1977. Lithostratigraphie et tectonique des schistes lustrés dans les Alpes cottiennes septentrionales et en Corse orientale. Mém. Inst. Géol., Univ. Louis Pasteur, Strasbourg, No. 48, 326 pp.

Clayton, R.N. and Mayeda, T.K., 1963. The use of bromine pentafluoride in the extraction of oxygen from oxides and silicates for isotopic analysis. Geochim. Cosmochim. Acta, 27: 43–52.

Clayton, R.N., O'Neil, J.R. and Mayeda, T.K., 1972. Oxygen isotope exchange between quartz and water. J. Geophys. Res., 77: 3057–3067.

Conolly, J.A. and Thompson, A.B., 1989. Fluid and enthalpy production during regional metamorphism. Contrib. Mineral. Petrol., 102: 347–366.

Cullers, R.L., Chaudhuri, S., Arnold, B., Lee, M. and Wolf, C.W., 1975. Rare earth distributions in clay minerals and in the clay-sized fraction of the Lower Permian Havensville and Eskridge shales of Kansas and Oklahoma. Geochim. Cosmochim. Acta, 39: 1691–1703.

Desmons, J., 1977. Mineralogical and petrological investigations of Alpine metamorphism in the internal French Western Alps. Am. J. Sci, 277: 1045–1066.

Desmons, J. and O'Neil, J.R., 1978. Oxygen and hydrogen isotope compositions of eclogites and associated rocks from the E Sesia Zone (W Alps, Italy). Contrib. Mineral. Petrol., 67: 79–85.

Ellenberger, F., 1958. Étude géologique du pays de Vanoise. Mém. Serv. Carte Géol. Fr., 562 pp.

Falconer, K., 1990. Fractal Geometry — Mathemetical foundations and Applications. Wiley, New York, N.Y.

Faure, G., 1986. Principles of Isotope Geology. Wiley, New York, N.Y.

Ferraris, G., Ivaldi, G. and Goffé, B., 1992. Structural study of a magnesian ferrocarpholite: Are carpholites monoclinic? Neues Jahrb. Mineral., Monatsh., 8: 337–347.

Ferry, J.M., 1980. A case study of the amount and distribution of heat and fluid during metamorphism. Contrib. Mineral. Petrol., 71: 373–385.

Ferry, J.M., 1986. Reaction progress: A monitor of fluid–rock interaction during metamorphic and hydrothermal events. In: J.V. Walther and B.J. Wood (Editors), Fluid–Rock Interactions during Metamorphism. Adv. Phys. Geochem., 5: 60–88.

Fleet, A.J., 1984. Aqueous and sedimentary geochemistry of the rare earth elements. In: P. Henderson (Editor), Rare Earth Element Geochemistry. Elsevier, Amsterdam, pp. 343–373.

Fletcher, R.C. and Hoffmann, A.W., 1974. Simple models of diffusion and combined diffusion–infiltration metasomatism. In: A.W. Hoffmann, B.J. Giletti, H.S. Yoder and R.A. Yund (Editors), Geochemical Transport and Kinetics. Carnegie Inst. Washington, D.C., Publ., 634: 243–260.

Floyd, P.A. and Winchester, J.A., 1978. Identification and discrimination of altered and metamorphosed volcanic rocks using immobile elements. Chem. Geol., 21: 291–306.

Frey, M., Hunziker, J.C., Frank, W., Bocquet, J., Dal Piaz, G.V., Jäger, E. and Niggli, E., 1974. Alpine metamorphism of the Alps — A review. Schweiz. Mineral. Petrogr. Mitt., 54: 247–290.

Frey, M., Hunziker, J.C., O'Neil, J.R. and Schwander, H.W., 1976. Equilibrium–disequilibrium relations in the Monte Rosa granite, Western Alps: Petrological, Rb–Sr and stable isotope data. Contrib. Mineral. Petrol., 55: 147–179.

Friedrichsen, H. and Morteani, G., 1979. Oxygen and hydrogen isotope studies on minerals from Alpine fissures and their gneissic host rocks, W Tauern Window (Austria). Contrib. Mineral. Petrol., 70: 149–152.

Früh-Green, G.L., Weissert, H. and Bernoulli, D., 1990. A multiple fluid history recorded in Alpine ophiolites. J. Geol. Soc. London, 147: 959–970.

Fyfe, W.S., Price, N.J. and Thompson, A.B., 1978. Fluids in the Earth's Crust. Elsevier, Amsterdam, 320 pp.

Gély, J.P., Létolle, R. and Loreau, J.P., 1989. Rapports isotopiques de l'oxygène des calcites comme marqueur diagénétique et stratigraphique dans les formations métamorphiques des Alpes de Savoie (France). C.R. Acad. Sci. Paris, 308: 1729–1735.

Gillet, Ph. and Goffé, B., 1988. On the significance of aragonite occurrences in the Western Alps. Contrib. Mineral. Petrol., 99: 70–81.

Goffé, B., 1977. Présence de cookéite dans les bauxites métamorphiques du Dogger de la Vanoise (Savoie). Bull. Soc. Fr. Minéral. Cristallogr., 100: 254–257.

Goffé, B., 1982. Définition du faciès à Fe-carpholite – chloritoïde, marqueur du métamorphisme de haute pression–basse température. Thèse d'État, Université Paris 6, Paris, 212 pp.

Goffé, B., 1996. Contribution à la carte métamorphique de la chaîne alpine: zonéographie du métamorphisme alpin des domaines non éclogitiques. Géol. Fr., Bur. Rech. Géol. Min. (submitted).

Goffé, B. and Chopin, C., 1986. High-pressure metamorphism in the Western Alps: zoneography of metapelites, chronology and consequences. Schweiz. Mineral. Petrogr. Mitt., 66: 41–52.

Goffé, B. and Velde, B., 1984. Contrasted metamorphic evolutions in thrusted cover units of the Briançonnais zone (French Alps): a model for the conservation of HP–LT metamorphic mineral assemblages. Earth Planet. Sci. Lett., 68: 351–360.

Goffé, B. and Vidal, O., 1992. Evidence for the controlling effect of the high-pressure metamorphic *P–T–t* path on the mass transfer of major elements. In: Y.K. Kharaka and A.S. Maest (Editors), Water–Rock Interaction. A.A. Balkema, Rotterdam, pp. 1499–1502.

Goffé, B. and Villey, M., 1984. Texture d'un matériel carboné impliqué dans un métamorphisme de haute pression–basse température (Alpes françaises) — Les hautes pressions influencent-elles la carbonification? Bull. Minéral., 107: 81–91.

Goffé, B., Murphy, W.M. and Lagache, M., 1987. Experimental transport of Si, Al and Mg in hydrothermal solutions: an application to vein mineralization during high-pressure, low-temperature metamorphism in the French Alps. Contrib. Mineral. Petrol., 97: 438–450.

Goffé, B., Michard, A., Garcia-Duenas, V., Gonzalez-Lodeiro, F., Monié, P., Campos, J., Galindo-Zaldivar, J., Jabaloy, A., Martinez-Martinez, J.M. and Simancas, J.F., 1989. First evidence of high-pressure, low-temperature metamorphism in the Alpujarride nappes, Betic Cordilleras (S.E. Spain). Eur. J. Miner., 1: 139–142.

Govindaraju, K., 1984. Compilation of working values and sample description for 170 international reference samples of mainly silicate rocks and minerals. Geostand. Newsl., 7: 3–16.

Graham, C.M., Greig, K.M., Sheppard, S.M.F. and Turi, B., 1983. Genesis and mobility of the H_2O–CO_2 fluid phase during regional greenschist and epidote amphibolite facies metamorphism: a petrological and stable isotope study in the Scottish Dalradian. J. Geol. Soc. London, 140: 577–599.

Graham, C.M., Harmon, R.S. and Sheppard, S.M.F., 1984. Experimental hydrogen isotope studies: hydrogen isotope exchange between amphibole and water. Am. Mineral., 69: 128–138.

Grambling, J.A., 1986. A regional gradient in the composition of metamorphic fluids in pelitic schists, Peços Baldy, New Mexico. Contrib. Mineral. Petrol., 94: 149–164.

Grant, J.A., 1986. The isocon diagram — A simple solution to Gresens' equation for metasomatic alteration. Econ. Geol., 81: 1976–1982.

Gray, D.R., Gregory, R.T. and Durney, D.W., 1991. Rock-buffered fluid–rock interaction in deformed quartz-rich turbidite sequences, eastern Australia. J. Geophys. Res., 96: 19681–19704.

Gregory, R.T. and Criss, R.E., 1986. Isotopic exchange in open and closed systems. In: J.W. Valley, H.P. Taylor, Jr. and J.R. O'Neil (Editors), Stable Isotopes in High Temperature Geological Processes. Mineral. Soc. Am., Rev. Mineral., 16: 91–127.

Gresens, R.L., 1967. Composition–volume relationships of metasomatism. Chem. Geol., 2: 47–55.

Haskin, L.A., Wildeman, T.R., Frey, F.A., Collins, K.A., Keedy, C.R. and Haskin, M.A., 1966. Rare earth in sediments. J. Geophys. Res., 71: 6091–6105.

Hoefs, J., 1987. Stable Isotope Geochemistry. Springer, Berlin, 241 pp.

Hoefs, J. and Frey, M., 1976. The isotopic composition of carbonaceous matter in a metamorphic profile from the Swiss Alps. Geochim. Cosmochim. Acta, 40: 945–951.

Hoernes, S. and Friedrichsen, H., 1974. Oxygen isotope studies on metamorphic rocks of the Western Hohe Tauern (Austria). Schweiz. Mineral. Petrogr. Mitt., 54: 769–788.

Hoernes, S. and Friedrichsen, H., 1978. Oxygen and hydrogen isotope study of the polymetamorphic area of the Northern Ötztal Stubai Alps. Contrib. Mineral. Petrol., 67: 305–315.

Hoernes, S. and Friedrichsen, H., 1980. Oxygen and hydrogen isotopic composition of Alpine and pre-Alpine minerals in the Swiss Central Alps. Contrib. Mineral. Petrol., 72: 19–32.

Hunziker, J.C., Frey, M., Clauer, N., Dallmeyer, R.D., Friedrichsen, H., Flehmig, W., Hochstrasser, K., Roggwiler, P. and Schwander, H., 1986. The evolution of illite to muscovite: mineralogical and isotopic data from the Glarus Alps, Switzerland. Contrib. Mineral. Petrol., 92: 157–180.

Jarvis, J.C., Wildeman, T.R. and Banks, N.G., 1975. Rare earths in the Leadville limestone and its marble derivates. Chem. Geol., 16: 27–37.

Jenner, G.A., Longerich, H.P., Jackson, S.E. and Fryer, B.J., 1990. ICP–MS — A powerful tool for high-precision trace-element analysis in Earth sciences: Evidence from analysis of selected U.S.G.S. reference samples. In: P.J. Potts, C. Dupuy and J.F.W. Bowles (Guest-Editors), Microanalytical Methods in Mineralogy and Geochemistry. Chem. Geol., 83: 133–148 (special issue).

Jullien, M. and Goffé, B., 1993. Occurrences de cookéite et de pyrophyllite dans les schistes du Dauphinois (Isère, France) — Conséquences sur la répartition du métamorphisme dans les zones externes alpines. Schweiz. Mineral. Petrogr. Mitt., 73: 357–363.

Keith, M.L. and Weber, J.N., 1964. Isotopic composition and environmental classification of selected limestones and fossils. Geochim. Cosmochim. Acta, 28: 1787–1816.

Kerrich, R., 1986. Fluid transport in lineaments. Philos. Trans. R. Soc. London, Ser. A, 317: 219–251.

Kerrich, R., 1987. Stable isotope studies of fluids in the crust. In: T.K. Kyser (Editor), Short Course in Stable Isotope Geochemistry of Low Temperature Fluids. Mineral. Assoc. Can., Short Course Handbk., 13: 258–286.

Kerrick, D.M., 1983. The $AlSiO_5$ Polymorphs. Mineral. Soc. Am., Rev. Mineral., Vol. 22, 406 pp.

Kullin, M. and Schmassmann, H., 1991. Isotopic composition of modern recharge. In: F.J. Pearson, W. Balderer, H.H. Loosli, B.E. Lehmann, A. Matter, T. Peters, H. Schmassmann and A. Gautschi (Editors), Applied Isotope Hydrogeology. Studies in Environmental Science, 43. Elsevier, Amsterdam, pp. 65–89.

Kyser, T.K., 1987. Equilibrium fractionation factors for stable isotopes. In: T.K. Kyser (Editor), Short Course in Stable Isotope Geochemistry of Low Temperature Fluids. Mineral. Assoc. Can., Short Course Handbk., 13: 1–84.

Kyser, T.K. and Kerrich, R., 1990. Geochemistry of fluids in tectonically active crustal regions. In: B.E. Nesbitt (Editor), Short Course on Fluids in Tectonically Active Regimes of the Continental Crust. Mineral. Assoc. Can., Short Course Handbk., 18: 133–230.

Lausch, J., Möller, P. and Morteani, G., 1974. Die Verteilung des seltenen Erden in den Karbonaten und penninischen Gneissen des zillertaler Alpen (Tirol, Österreich). Neues Jahrb. Mineral., Monatsh., 11: 490–507.

Lemoine, M., Bourbon, M., de Graciansky, P.C. and Létolle, R., 1983. Isotopes du carbone et de l'oxygène de calcaires associés à des ophiolites (Alpes Occidentales, Corse, Apennin): indices possibles d'un hydrothermalisme océanique téthysien. Rev. Géol. Dyn. Géogr. Phys., 24: 305–314.

McCaig, A.M., 1984. Fluid–rock interaction in some shear zones from the central Pyrenees. J. Metam. Geol., 2: 129–141.

McCaig, A.M., 1988. Deep fluid circulation in fault zones. Geology, 16: 867–870.

McCaig, A.M., Wickham, S.M. and Taylor, H.P., 1990. Deep fluid circulation in Alpine shear zones, Pyrenees, France: field and oygen isotope studies. Contrib. Mineral. Petrol., 106: 41–60.

McCrea, J.M., 1950. The isotope chemistry of carbonates and a paleotemperature scale. J. Chem. Phys., 18: 849–857.

McGillavry, C.H., Korst, W.L., Moore, W. and van der Plas, E.J., 1956. The crystal structure of ferrocarpholite. Acta Crystallogr., 9: 773–776.

Marquer, D. and Burkhard, M., 1992. Fluid circulation, geochemical mass transfer and progressive deformation in the upper crust: examples of basement–cover relationships in the external crystalline massifs (central Alps Switzerland). J. Struct. Geol., 14: 1047–1057.

Michard, A. and Henry, C., 1988. Les nappes briançonnaises en Haute Ubaye (Alpes franco-italiennes): contribution à la reconstruction paléogéographique du Briançonnais au Mésozoïque. Bull. Soc. Géol. Fr., 4: 693–701.

Nelson, B.K., 1991. Sediment-derived fluids in subduction zones: Isotopic evidence from veins in blueschist and eclogite of the Franciscan Complex, California. Geology, 19: 1033–1036.

Nystrom, J.O., 1984. Rare earth element mobility in vesicular lava during low-grade metamorphism. Contrib. Mineral. Petrol., 88: 328–331.

Oliver, J., 1992. The spots and stains of plate tectonics. Earth-Sci. Rev., 32: 77–106.

O'Neil, J.R., Clayton, R.N. and Mayeda, T.K., 1969. Oxygen isotope fractionation in divalent metal carbonates. J. Chem. Phys., 51: 5547–5558.

Petersen, M.D., 1983. The use of the "immobile" elements Zr and Ti in lithogeochemical exploration for massive sulphide deposits in the Precambrian Peços greenstone belt of northern New Mexico. J. Geochem. Explor., 19: 615–617.

Philippot, P. and Selverstone, J., 1991. Trace-element-rich brines in eclogitic veins: implications for fluid composition and transport during subduction. Contrib. Mineral. Petrol., 106: 416–430.

Ramsay, J.G. and Huber, M., 1983. The Techniques of Modern Structural Geology, Vol. 1: Strain Analysis. Academic Press, London, 307 pp.

Roaldset, E., 1975. Rare earth elements distributions in some Precambrian rocks and their phyllosilicates, Numedal, Norway. Geochim. Cosmochim. Acta, 39: 455–469.

Roure, F., Polino, R. and Nicolich, R., 1990. Neogene deformation beneath the Po plain: constraints on post-collisional Alpine evolution. In: F. Roure, P. Heitzmann and R. Polino (Editors), Deep Structure of the Alps. Mém. Soc. Géol. Fr., 156; Mém. Soc. Géol. Suisse, 1; Vol. Spec. Soc. Geol. Ital., 1: 309–321.

Rumble, D. and Spear, F.S., 1983. Oxygen-isotope equilibration and permeability enhancement during regional metamorphism. J. Geol. Soc. London, 140: 619–628.

Saliot, P., 1973. Les principales zones de métamorphisme dans les Alpes françaises — Répartition et signification. C.R. Acad. Sci. Paris, 276: 3081–3084.

Savin, S.M. and Epstein, S., 1970. The oxygen and hydrogen isotope geochemistry of clay minerals. Geochim. Cosmochim. Acta, 34: 25–42.

Sharp, Z.D., Essene, E.J. and Hunziker, J.C., 1993. Stable isotope geochemistry and phase equilibria of coesite-bearing whiteschists, Dora Maira Massif, Western Alps. Contrib. Mineral. Petrol, 114: 1–12.

Sheppard, S.M.F, 1986. Characterization and isotopic variations in natural waters. In: J.W. Valley, H.P. Taylor, Jr., J.R. O'Neil (Editors), Stable isotopes in high temperature geological processes. Mineral. Soc. Am., Rev. Mineral., 16: 165–183.

Steen, D. and Bertrand, J., 1977. Sur la présence de ferrocarpholite associée aux schistes à glaucophane de Haute-Ubaye (Basses-Alpes, France). Schweiz. Mineral. Petrogr. Mitt., 57: 157–168.

Suzuoki, T. and Epstein, S., 1976. Hydrogen isotope fractionation between OH-bearing minerals and water. Geochim. Cosmochim. Acta, 40: 1229–1240.

Taylor, S.R. and McLennan, S.M., 1985. The Continental Crust: Its Composition and Evolution. Blackwell, Oxford, 312 pp.

Vidal, O. and Goffé, B., 1991. Cookeite $LiAl_4(Si_3Al)O_{10}(OH)_8$: Experimental study and thermodynamical analysis of its compatibility relations in the Li_2O–Al_2O_3–SiO_2-H_2O system. Contrib. Mineral. Petrol., 108: 72–81.

Vidal, O., Goffé, B. and Theye, T., 1992. Experimental study of the stability of sudoite and magnesiocarpholite and calculation of a new petrogenetic grid for the system FeO–MgO–Al_2O_3–SiO_2–H_2O. J. Metam. Geol., 10: 603–614.

Viswanathan, K., 1981. The crystal structure of an Mg-rich carpholite. Am. Mineral., 66:1080–1085.

Wedepohl, K.H., 1978. Handbook of Geochemistry. Springer, Berlin, 5 vols.

Weiss, L.E., 1972. The Minor Structures of Deformed Rocks. Springer, Berlin, 431 pp.

Weissert, H. and Bernoulli, D., 1984. Oxygen isotope composition of calcite in Alpine ophicarbonates: a hydrothermal or Alpine metamorphic signal? Eclogae Geol. Helv., 77: 29–43.

Wenner, D.B. and Taylor, H.P., 1971. Temperatures of serpentinization of ultramafic rocks based on $^{18}O/^{16}O$ fractionation between coexisting serpentine and magnetite. Contrib. Mineral. Petrol., 32: 165–185.

Wenner, D.B. and Taylor, H.P., 1973. Oxygen and hydrogen isotopic studies in the serpentinization of the ultramafic rocks in oceanic environments and continental ophiolitic complexes. Am. J. Sci., 273: 207–239.

Wood, B.J. and Walther, J.V., 1986. Fluid flow during metamorphism and its implications for fluid–rock ratios. In: J.V. Walther and B.J. Wood (Editors), Fluid–Rock Interactions during Metamorphism. Adv. Phys. Geochem., 5: 89–108.

Yardley, B.W.D., 1983. Quartz veins and devolatilization during metamorphism. J. Geol. Soc. London, 140: 657–663.

Yardley, B.W.D., 1986. Fluid migration and veining in the Connemara Schists, Ireland. In: J.V. Walther and B.J. Wood (Editors), Fluid–Rock Interactions during Metamorphism. Adv. Phys. Geochem., 5: 109–131.

Yardley, B.W.D. and Botrell, S.H., 1992. Silica mobility and fluid movement during metamorphism of the Connemara schists, Ireland. J. Metam. Geol., 10: 453–465.

Zheng, Y.F., 1991. Calculation of oxygen isotope fractionation in metal oxides. Geochim. Cosmochim. Acta, 55: 2299–2307.

Zheng, Y.F., 1993a. Calculation of oxygen isotope fractionation in anhydrous silicate minerals. Geochim. Cosmochim. Acta, 57: 1079–1091.

Zheng, Y.F., 1993b. Calculation of oxygen isotope fractionation in hydroxyl-bearing silicates. Earth Planet. Sci. Lett., 120: 247–263.

Zielinski, R.A., 1985. Element mobility during alteration of silicic ash to kaolinite — a study of tonstein. Sedimentology, 32: 567–579.